Strengthening of concrete structures with ultra high performance fiber reinforced concrete (UHPFRC)
A critical review

Huang, Yitao; Grunewald, Steffen ; Schlangen, Erik; Lukovic, Mladena

DOI
10.1016/j.conbuildmat.2022.127398

Publication date
2022

Document Version
Final published version

Published in
Construction and Building Materials

Construction and Building Materials 336 (2022) 127398

Contents lists available at ScienceDirect

Construction and Building Materials

journal homepage: www.elsevier.com/locate/conbuildmat

Review

Strengthening of concrete structures with ultra high performance fiber reinforced concrete (UHPFRC): A critical review

Yitao Huang [a,*], Steffen Grünewald [a,b], Erik Schlangen [c], Mladena Luković [a]

[a] Engineering Structures, Delft University of Technology, Stevinweg 1, Delft 2628 CN, the Netherlands
[b] Department Structural Engineering and Building Materials, Ghent University, Technologiepark-Zwijnaarde 60, Ghent 9052, Belgium
[c] Microlab, Faculty of Civil Engineering and Geosciences, Delft University of Technology, Delft 2628 CN, the Netherlands

ARTICLE INFO

Keywords:
Ultra-high performance fiber-reinforced concrete (UHPFRC)
Strengthening
UHPFRC hybrid concrete structures
Interface performance
Modelling
Design codes

ABSTRACT

Ultra-High Performance Fiber-Reinforced Concrete (UHPFRC) is, due to its superior mechanical properties and low permeability, a promising material for the restoration and improvement of the mechanical resistance and durability of existing Reinforced Concrete (RC) structures. This paper reviews the strengthening applications of UHPFRC in flexure, shear and punching shear, with a focus on shear performance of hybrid structures and the UHPFRC-concrete interface behavior which is governing the response of the hybrid beams. Holistic review approach is adopted considering not only structural behaviour of hybrid UHPFRC-concrete beams at the macro-scale, but also parameters governing the interface behaviour between concrete and UHPFRC at the meso- and micro-scale. Current analytical and numerical methods to predict the shear or punching shear capacity of RC structures strengthened with UHPFRC are reviewed and critically analyzed. Furthermore, the frequently overlooked role of interface, the effects of bonding technique, moisture exchange between the two materials, differential shrinkage and the role of coupled environmental and mechanical loads are discussed. It is observed that although extensive research work has been conducted to study the performance of hybrid UHPFRC-concrete structures, poor understanding of the behavior at the interface between concrete and UHPFRC, the role of thermal and hygral gradients and stress concentration for premature debonding, and the lack of reliable models and design codes impede the wide application of UHPFRC.

1. Introduction

Due to increase of loads, natural environmental deterioration mechanisms and more stringent requirements in design codes, the bearing capacity of existing concrete structures decreases and/or does no longer satisfy service demands. Reconstruction and rehabilitation are the two main methods to improve structural resistance. Rehabilitation usually implies a repair/strengthening process to upgrade the strength or to improve the durability and therefore extend the service life of existing structures. Compared to reconstruction, which is usually related to construction activities to replace the deteriorated structures, rehabilitation is usually preferred by government and industry. Advantages include shorter 'out-of-use periods' of structure, less traffic hindrance and cost effectiveness [1]. A common strengthening measure is to cast a layer of new concrete in the regions where principal stresses are the largest to improve structural resistance. However, structures strengthened with normal concrete (NC) can suffer a decrease in their resistance again after only a short time [2]. This issue prompted researchers to look into the application of advanced cementitious materials for strengthening of structural concrete elements.

UHPFRC is a relatively new construction material with high compressive and tensile strength, as well as superior durability that is attractive for strengthening applications. Compared to normal concrete, UHPFRC has a dense and compact microstructure with low permeability due to the use of fine particles like silica fume, a low water-binder ratio and the addition of superplasticizer [3]. Consequently, UHPFRC shows high resistance against degradation processes such as ingress of carbon dioxide, chloride, sulfate and corrosive liquids [4-6], and damage due to freeze-thaw cycles and thermal loads [7]. The low amount of coarse aggregates (in size and volume) and a high fiber content (normally 2 or 3% by volume) cause increased strength, stiffness and ductility. Moreover, its excellent rheological properties facilitate casting when the

* Corresponding author.
E-mail addresses: Y.Huang-6@tudelft.nl (Y. Huang), S.Grunewald@tudelft.nl (S. Grünewald), Erik.Schlangen@tudelft.nl (E. Schlangen), M.Lukovic@tudelft.nl (M. Luković).

https://doi.org/10.1016/j.conbuildmat.2022.127398
Received 8 September 2021; Received in revised form 13 March 2022; Accepted 4 April 2022
Available online 22 April 2022

material is in the fresh state [8]. In terms of compressive strength, UHPFRC must have a characteristic cylinder compressive strength of at least 150 MPa, which is significantly higher than that of NC (less than 50 MPa). UHPFRC also has higher tensile strength and shows strain (or deflection) hardening behavior due to the effect of fibers, subsequently accompanied by a softening plateau and pullout of the fibers. Therefore, multiple cracks will be developing until a localized macrocrack opens, which results in ductile behavior of UHPFRC and significantly higher fracture energy compared to NC. In addition, the embedded fibers also make UHPFRC a high confining effect to resist the spalling of the matrix and UHPFRC becomes a promising material to resist blast/impact loads due to its outstanding energy absorption capacities [9].

The application of UHPFRC is increasing worldwide. UHPFRC-application can be categorized into construction of new lightweight structures and strengthening of existing structures [8]. In Europe, Australia and North America with advanced UHPFRC technologies, UHPFRC is mainly applied in bridge components, including repair/rehabilitation of deck and piers [10-12], cast in-place/precast girders [13], and construction of joints of prefabricated elements [14], as well as slender and architectural building elements [15,16]. In Asian countries like Malaysia, UHPFRC has been largely used in view of great demand for infrastructure and durability problems. In Malaysia alone, there are more than 200 UHPFRC road bridges constructed or are under construction to date [17]. In addition to concrete structures, UHPFRC application is also extended to strengthen the orthotropic steel decks in Netherlands and China [18,19]. Detailed overviews of new UHPFRC structures and its strengthening applications are provided in literature [20-28].

As listed before, UHPFRC is a promising material with numerous qualities, but a few shortcomings still limit its wide practical application: immature construction technology, scatter in material properties, lack of design codes, and high material price, among others [24]. Though efforts have been made to establish design standards such as AFGC [29] and JSCE [30] to facilitate the application of UHPFRC, most of available codes focus on the material properties characterization and design of new UHPFRC structures. Provisions on UHPFRC strengthening technologies are only available in the Swiss norm (SIA 2016) [31] but still limited, which restrains its wide strengthening applications. UHPFRC is nowadays applied more often since UHPFRC can replace NC to satisfy the design requirements, especially when strength, durability and aesthetics are the main concern for the stakeholders. It has to be noted that although the higher cement content in UHPFRC compared to NC increases the CO_2 footprint of the material itself, the superior performance of UHPFRC may enable the longer service life [32], the construction of slender structures, reduction of traffic hindrance [33] and can greatly reduce the needed amount of construction material, resulting in improved sustainability aspects [34]. Furthermore, in spite of higher material costs, the overall construction cost when UHPFRC is applied (Strategy A) is not more or even less expensive than that of NC as strengthening material (Strategy B) when reduction of material demand and traffic intervention, the long-term serviceability and decrease of future maintenance are taken into account, contributing to a great potential for benefits (Fig. 1 [2]).

The aim of this paper is to review current UHPFRC-applications as a strengthening material. Particular focus is directed on the interface behavior between UHPFRC and NC which is governing the behavior of the strengthening system. In view of this, the behavior of UHPFRC-concrete hybrid structures [35-41], both considering new hybrid systems, and strengthening of existing reinforced concrete structures with UHPFRC, is investigated. Strengthening mechanisms in flexure, shear and punching shear, and some typical construction practices are discussed. With regard to interface behavior, bond strength test methods to evaluate the interface strength are summarized. The effect of different parameters including the bonding technique, moisture exchange between two materials, differential shrinkage, and coupled environmental and mechanical loads on the interfacial performance are analyzed.

2. Strengthening applications of UHPFRC

2.1. Flexural strengthening

Due to its relatively large tensile strength (>7MPa) and extremely high toughness, UHPFRC is usually applied as an overlay with an appropriate thickness on the tension zone of NC elements to improve the flexural resistance or durability. In general, three configurations have been proposed by Brühwiler and Denarié [11] (Fig. 2). In the first and second configurations, a thin layer of UHPFRC (about 20 to 30 mm) is mainly used to protect the existing structure from ingress of water or detrimental chemicals. In the second configuration, the original deteriorated concrete together with embedded rebars is removed and new rebars are integrated in the UHPFRC, which is important for durability of the strengthened structures. The third configuration improves the flexural resistance of an existing structure by applying a layer of 40 to 70 mm UHPFRC together with additional rebars. A state-of-the-art of

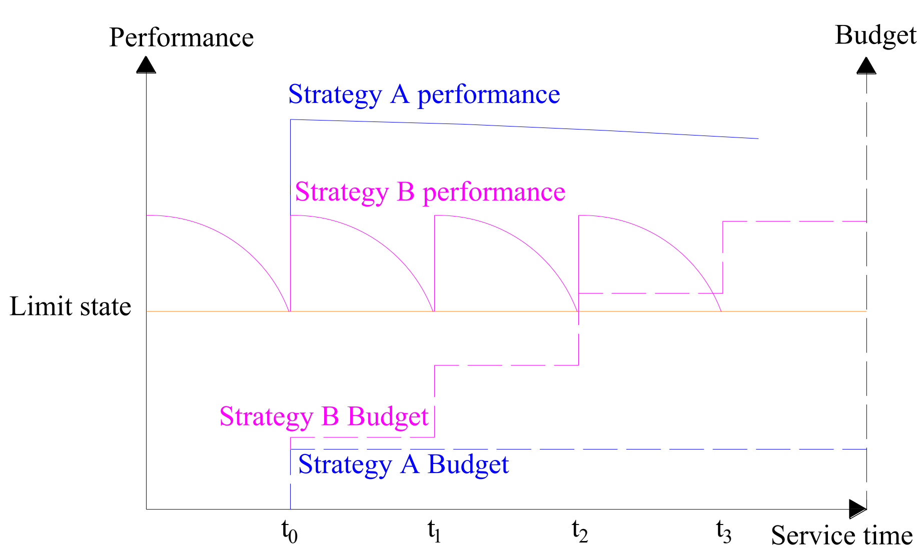

Fig. 1. Two different strengthening strategies for service life maintenance: Strategy A (Structures strengthened with UHPFRC and Strategy B (Structures strengthened with NC) [2].

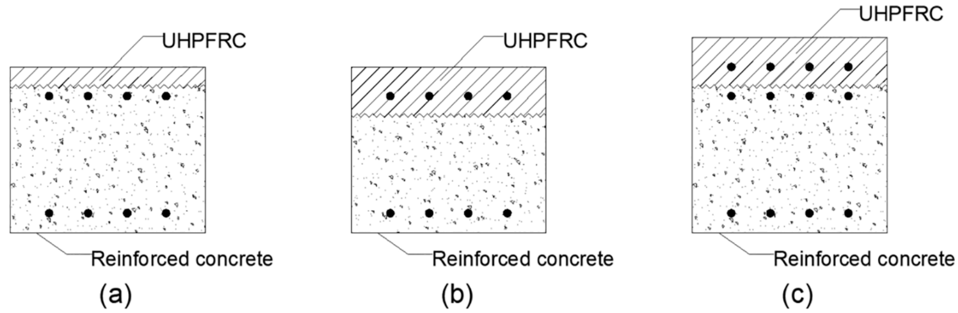

Fig. 2. Concept and principle of composite structural element when UHPFRC layer has a protection function, (**a**) without and (**b**) with reinforcement embedded in; and (**c**) when UHPFRC is used for strengthening, both providing protective function and improving structural resistance [11].

strengthening in flexure with UHPFRC has been performed by Zhu [42]. Given this extensive overview by Zhu [42], current review addresses merely one large-scale application of UHPFRC for flexural strengthening, focusing on interface performance.

In 2012, Chillon viaducts were diagnosed with alkali-activated reaction which reduced their load bearing capacity [43]. Application of UHPFRC combined with rebars (Fig. 2c) was chosen as the most effective mean to strengthen Chillon viaducts. The concrete substrate was prepared by high pressure water jetting. No debonding was observed under the action of pure bending [36,44-47]. The composite behaved monolithically and the maximum bending resistance was calculated under the assumption of plane section [43,48]. For a specific application, Brühwiler et al. [43] predicted a 73% increase of the bending resistance of the composite beam compared to the capacity of the existing, undamaged cross-section.

2.2. Shear strengthening

Conventionally, a reinforced NC jacket has been applied to increase the cross section area for improving the shear resistance [49]. In order to reduce the additional self-weight load from the NC jacket, while realizing the same improvement, application of the UHPFRC jacket, due to its high tensile strength, can be an effective strengthening method. Until now there still exist some difficulties for practical shear strengthening application with UHPFRC such as the low workability of large amount UHPFRC production, high autogenous shrinkage as well as construction difficulty. However, it is worthwhile to explore the potential of UHPFRC as a strengthening material for shear-deficient concrete structures from laboratory studies, which pave a foundation for more on-site practice in future.

Only a few experimental studies have been carried out to investigate the shear performance of UHPFRC strengthened beams. These studies investigated the influence of UHPRFC thickness, the amount of rebars, and strengthening configurations. An overview of different experimental studies on the shear capacity of high performance fiber reinforced concrete (HPFRC) or UHPFRC strengthened RC structures is given in Table 1 [47,50-53], while typical shear strengthening configurations are shown in Fig. 3. Note that although configuration 3a is usually used for flexural strengthening, the authors from presented studies used this configuration to study the shear capacity improvement. Therefore, this configuration is included in the overview.

Based on the experimental database summarized in Table 1, the effect of (a) concrete substrate strength, (b) steel fiber content in UHPFRC, (c) reinforcement in UHPFRC, (d) strengthening configuration and (e) connection method, and (f) shear-span ratio on the beam shear capacity have been analyzed and presented respectively in Fig. 4(a), 4(b), 4(c), 4 (d), 4(e), 4(f). The effects of abovementioned parameters on the shear capacity of the composite beams and the strengthening effect have been evaluated through the following equation:

$$\textit{Increase in shear resistance}\,(\%) = \left(\frac{V}{V_{con}} - 1\right) \times 100, \tag{1}$$

where V represents the shear capacity of the strengthened beam, V_{con} represents the shear capacity of the control beam.

First the effect of compressive strength of the parent concrete on the shear improvement when UHPFRC is added is analyzed. NC control beam and High strength concrete (HSC) control beam were compared with the hybrid beams in which a part of parent concrete is replaced by UHPFRC. The hybrid beams show 60–110% enhancement of shear capacity (Fig. 4(a)) compared to control beams, irrespectively of the concrete compressive strength of parent concrete. The relationship between steel fiber content and the increase of shear resistance of concrete beams is shown in Fig. 4(b). Theoretically, the shear capacity of a beam with fiber reinforcement [54] will increase as more fibers would bridge the shear crack. However, the effect of the steel fiber content on the shear capacity of composite beams is unclear (Fig. 4(b)), which is similar to findings of Jongvivatsakul et al. [55]. Still Mohammed et al. [47] reported that the crack width growth is greatly restricted due to the increased amounts of fibers. The reinforcement in UHPFRC and the strengthening configuration will also influence the shear resistance of strengthened beams (Fig. 4(c) and (d)). Longitudinal rebars will increase the shear resistance due to the dowel action (Fig. 4(c)). In terms of strengthening configuration, 2-sided strengthening resulted in greater shear capacity increase in comparison with the same corresponding thickness L-sided strengthening, and, as expected, shear resistance is only slightly increased from 2-sided to 3-sided strengthening (Fig. 4(d)). However, from Table 1, it should be noted that the failure modes with different strengthening schemes change from shear to flexure [50], and therefore the actual increase of shear resistance is higher than the capacity shown in Fig. 4(d). Assessing the increase of the shear capacity when the type of failure is changing to e.g. flexural failure is not appropriate since it only presents the lower bound value. The strengthening effect of different bonding techniques (cast in-situ and two forms of mechanical anchorage) is also analyzed and compared in Fig. 4(e): the interface produced with different techniques does not affect the shear capacity of the strengthened beam as long as the interface strength is high enough to resist the debonding until failure. However, from Table 1, it can be observed that some beams also failed due to debonding, thus answers have to be provided on how to characterize the interface performance and to evaluate its effect on the capacity. Finally the role of shear-span (a/d) ratio is investigated (Fig. 4 (f)). The capacity improvement reduces as the shear-span (a/d) ratio increases from around 1 to 3. To conclude, the knowledge on underlying mechanisms such as the role of interface, type of the bond and fiber contribution are lacking and more accurate methods for characterization and evaluation of the shear resistance improvement still need to be developed.

Table 1
Overview of test results for beams strengthened in shear.

Reference	Specimen name	Dimension $b \times h \times L$ (mm)	Fibers Vol.-%	Strengthening technique	Strengthening pattern: Configuration	Strengthening pattern: UHPFRC thickness (mm)	a/d ratio	Cracking load (kN)	Failure load (kN)	Deflection at failure load (mm)	Failure type
Hussein et al. [47]	NS1	150×300×1584	–	–	–	–	3	165	250.84	4.63	Shear
	UNS2-1	150×300×1584	1	Cast in-situ	T-sided	150	3	295	436.24	6.15	Shear
	UNS2-1D	150×300×1584	1	Dowel connection	T-sided	150	3	300	402.25	5.55	Shear
	UNS2-1S	150×300×1584	1	Shear stud connection	T-sided	150	3	300	430.24	6.46	Shear
	UNS2-1.5	150×300×1584	1.5	Cast in-situ	T-sided	150	3	310	439.15	7.66	Shear
	UNS2-1.5D	150×300×1584	1.5	Dowel connection	T-sided	150	3	280	503.56	6.41	Shear
	UNS2-2	150×300×1584	2	Cast in-situ	T-sided	150	3	350	521.56	6.63	Shear
	UNS2-2D	150×300×1584	2	Dowel connection	T-sided	150	3	310	502.45	7.24	Shear
	HS1	150×300×1584	–	–	–	–	3	160	256.61	4.62	Shear
	UHS2-1	150×300×1584	1	Cast in-situ	T-sided	150	3	280	528.41	8.57	Shear
	UHS2-1D	150×300×1584	1	Dowel connection	T-sided	150	3	280	439.22	9.52	Shear
	UHS2-1S	150×300×1584	1	Shear stud connection	T-sided	150	3	290	433.02	6.19	Shear
	UHS2-1.5	150×300×1584	1.5	Cast in-situ	T-sided	150	3	245	403.59	5.15	Shear
	UHS2-1.5D	150×300×1584	1.5	Dowel connection	T-sided	150	3	290	465.79	6.52	Shear
	UHS2-2	150×300×1584	2	Cast in-situ	T-sided	150	3	300	522.89	6.45	Shear
	UHS2-2D	150×300×1584	2	Dowel connection	T-sided	150	3	370	521.45	10.92	Shear
Bahraq et al. [50]	CT-1.0	140×230×1120	–	–	–	–	1	–	383	2.17	Shear
	SB-2SJ-1.0	200×230×1120	2	Cast in-situ	2-sided	30	1	–	567	3.47	Flexure-shear
	SB-3SJ-1.0	200×260×1120	2	Cast in-situ	3-sided	30	1	–	628	3.10	Flexure
	CT-1.5	140×230×1120	–	–	–	–	1.5	–	286	4.40	Shear
	SB-2SJ-1.5	200×230×1120	2	Cast in-situ	2-sided	30	1.5	–	402	5.20	Flexure-shear
	SB-3SJ-1.5	200×260×1120	2	Cast in-situ	3-sided	30	1.5	–	482	4.10	Flexure
	CT-2.0	140×230×1120	–	–	–	–	2	–	276	7.00	Shear
	SB-2SJ-2.0	200×230×1120	2	Cast in-situ	2-sided	30	2	–	346	7.50	Flexure-shear
	SB-3SJ-2.0	200×260×1120	2	Cast in-situ	3-sided	30	2	–	353	4.14	Flexure
Garg et al. [51]	CB-U/R	150×150×700	–	–	–	–	1.6	32	123	3.422	Shear
	UT-U/R	150×150×700	2	Cast in-situ	3-sided	25	1.6	38.25	157.9	8.424	Flexure
	EJ-U/R	200×150×700	2	Cast in-situ	2-sided	25	1.6	39.25	115.75	1.83	Debonding
	CB-O/R	150×150×700	–	–	–	–	1.6	48	140	4.525	Shear
	UT-O/R	150×150×700	2	Cast in-situ	3-sided	25	1.6	56.6	174	8.273	Flexure
	EJ-O/R	200×150×700	2	Cast in-situ	2-sided	25	1.6	55.2	131.375	2.689	Debonding
A. Sakr et al. [52]	C-S	150×300×2000	–	–	–	–	2	48	115	5.35	Shear
	C-F	150×300×2000	–	–	–	–	2	70	253	15.77	Flexure
	C-S-210	210×300×2000	–	–	–	–	2	58	211	7.11	Shear
	ST-2S	210×300×2000	2	EB	2-sided	30	2	93	281	8.23	Flexure
	ST-1S	210×300×2000	2	EB	L-sided	60	2	60	153	7.25	Shear
	ST-2S-R	210×300×2000	2	EB and AC	2-sided	30	2	110	331	10.31	Flexure
	ST-1S-R	210×300×2000	2	EB and AC	L-sided	60	2	64	252	6.79	Shear
Ji et al. [53]	RC-2.7	200×500×2700	–	–	–	–	2.7	–	655	–	Shear
	RC-U-2.7	200×550×2700	2.5	–	T-sided	50	2.7	–	717	–	Shear
	RC-RU-2.7	200×550×2700	2.5	–	T-sided	50	2.6	–	922	–	Shear
	RC-RU-2.4	200×550×2400	2.5	EB	T-sided	50	2.2	–	955	–	Shear
	RC-RU-3.1	200×550×3100	2.5	EB	T-sided	50	3.2	–	761	–	Shear

Noted: EB denotes epoxy bonded and AC denotes anchorage connection.

2.3. Punching shear strengthening

Casting UHPFRC layers with or without small diameter steel rebars in RC slabs has been proposed as an innovative strengthening technique to improve the structural punching shear resistance. Both experimental research and theoretical models are adopted to study the shear punching resistance of RC slabs strengthened by UHPFRC [37,39,56-59]. The effect of parameters such as the thickness of the UHPFRC layer, the amount of reinforcement inserted in UHPFRC and strengthening configuration were analyzed. Experimental results in [37] showed that a 50 mm thick layer of UHPFRC increases the punching resistance of the RC slab by at least 69% without decreasing its rotational capacity [37]. A first composite model was developed by Bastien-Masse [56] and then modified [58] to calculate the force-rotation relationship and the punching shear resistance of composite R-UHPFRC-reinforced concrete slabs [37]. Mechanisms of resistance of UHPFRC to punching shear resistance are shown in Fig. 5. A layer of UHPFRC in the tension section of a slab has been found to contribute to the punching shear resistance dependent on the concrete tensile strength f_{ct}. Due to high tensile strength of UHPFRC, it will hinder the opening of the punching shear crack to cross the UHPFRC layer and thus UHPFRC layer is compatible to movement of the RC slab by bending out-of-plane in double curvature. Afterwards, a horizontal crack near interface between UHPFRC and normal concrete will initiate and propagate until final punching shear

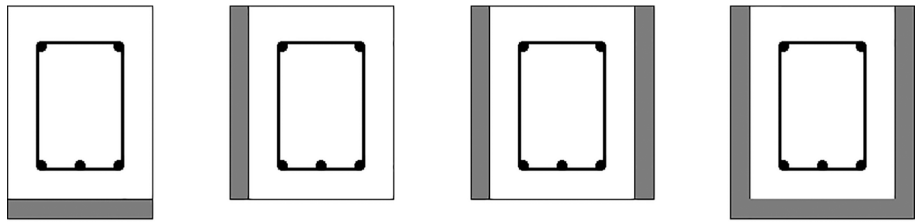

(a) (b) (c) (d)

Fig. 3. Typical patterns for shear strengthening with UHPFRC (a) T-sided (Strengthening on tension side); (b) L-sided (Strengthening on one lateral side); (c) 2-sided (Strengthening on two lateral sides); (d) 3-sided beam (Strengthening on three sides).

occurs.

One case of punching shear improvement with UHPFRC is in a massive RC slab bridge with six supporting columns built in 1963. This bridge was found to have insufficient loading capacity due to the increase of vehicle load and deterioration of the deck slab [60]. A 65 mm thick R-UHPFRC layer was cast below the existing deck in area around the columns to both increase the bending and punching shear resistance (Fig. 6).

3. Modeling of concrete beams and slabs strengthened with UHPFRC

The lack of design codes, among others, impedes the growth of UHPFRC strengthening applications. Effective analytical and numerical methods to predict the performance of such composite structures are of great importance for enabling practical applications of the developed techniques.

A summary of calculation methods for evaluating the flexural performance of UHPFRC-NC structures is given in [42]. The following two assumptions are generally made: (1) Plain sections remain plain in bending; (2) A perfect bond exists between UHPFRC and RC and the slip is neglected at the interface. It is concluded that the predicted cracking and ultimate bending moments based on the proposed methods for flexural improvement agree well with the laboratory tested data.

In this paper we focus on an overview of current modeling methods for shear or punching shear capacity of UHPFRC-NC structures. An overview of analytical and/or numerical results compared to experimental results in terms of the shear resistance is given in Table 2. Note that Yin et al. [61] gives six methods based on existing standards and the ratio presented in Table 2 denotes results from method A3 based on JSCE-2007 (2010) [62]; the results predicted by Ji et al. [53] are based on the ultimate equilibrium theory. As shown in Table 2, the numerically predicted shear resistance and fracture pattern in FE modelling agree well with experimental results; however, the predicted shear capacities from different analytical models deviate greatly from experimental values.

3.1. Analytical modeling of shear and punching shear resistance

3.1.1. Analytical models for shear resistance

From the available shear analytical models in current codes, two concepts are classified for shear strength evaluation [61]. The first concept points that the shear strength of composite structures is the sum of independent contributions from the RC part and the UHPFRC layer:

$$V_R = V_{UHPFRC} + V_{RC} \tag{2}$$

where V_R, V_{UHPFRC}, V_{RC} represent the shear resistance of composite structure, the UHPFRC layer and the RC part, respectively. This concept is based on two assumptions: (1) The RC component and the UHPFRC layer fail simultaneously; (2) The effect of the weak interface between UHPFRC and RC is neglected. For the original RC part, the shear load is mainly carried by the concrete in the compression zone and the stirrups, and current design codes ACI 318 (2008) [64], EN 1992-1-1 (2004) [65], and JSCE-2007 (2010) [62] give corresponding equations for shear resistance calculations. For V_{UHPFRC} component, two methods are used to calculate the contribution of UHPFRC:

(1) As done in ACI 544 (1988) [66] and MC 2010 (2010) [67], shear contribution of UHPFRC is addressed without separating effect of fibers and matrix. Similarly, Noshiravani and Brühwiler [68,69] and Masse and Brühwiler [70] proposed a composite hinge model for flexure shear resistance of T-sided reinforced beams with reinforced UHPFRC. Nonlinear interfacial behavior between UHPFRC and RC is considered and the shear resistance of the R-UHPFRC element in double bending is determined through hinge rotation. Based on the proposed equation for cantilever beam by Noshiravani and Brühwiler [68], Ji and Liu [53] extended the calculation method for UHPFRC-NC simple supported composite beams with stirrups considering the size effect.
(2) As done in Japan Society of Civil Engineers (JSCE) [30] and French Society of Civil Engineers (AFGC) codes [29], the shear resistance of UHPFRC is obtained by separating the shear contribution from cement matrix and fiber. The concept is denoted as:

$$V_{UHPFRC} = V_c + V_f \tag{3}$$

where V_c and V_f represent the shear resistance from the matrix and fibers in UHPFRC layer respectively. Inspired by the second method, Hussein and Amleh [47] proposed an analytical model describing that shear resistance of a UHPFRC-NSC/HSC beam without shear reinforcement is equal to the shear resistance provided by the concrete in the compression zone and fibers. This analytical model was validated by experimental results, as indicated in Table 2.

The second concept considers the shear contribution from steel fibers as the equivalent longitudinal rebar ratio. Thus, the calculated total ratio ρ is equal to:

$$\rho = \rho_s + \rho_{eq,F} \tag{4}$$

where ρ_s is the rebar ratio in RC part and given as $\rho_s = \frac{A_s}{bwd}$. $\rho_{eq,F}$ is the equivalent longitudinal rebar ratio and can be calculated as:

$$\rho_{eq,F} = Vol. - \% \left(\frac{f_{ct}}{f_y}\right)\left(\frac{A_{UHPFRC}}{A_{RC}}\right) \tag{5}$$

where f_{ct} is the tensile stress of UHPFRC; f_y is the yield strength of the longitudinal rebar; A_{UHPFRC} and A_{RC} are the areas of the UHPFRC and RC part, respectively; and $Vol.-\%$ is the volume ratio of steel fibers.

3.1.2. Analytical models for punching shear resistance

Only a few studies have focused on establishing analytical models for punching shear to assess the performance of slab strengthened with UHPFRC. In order to predict the punching shear resistance of R-

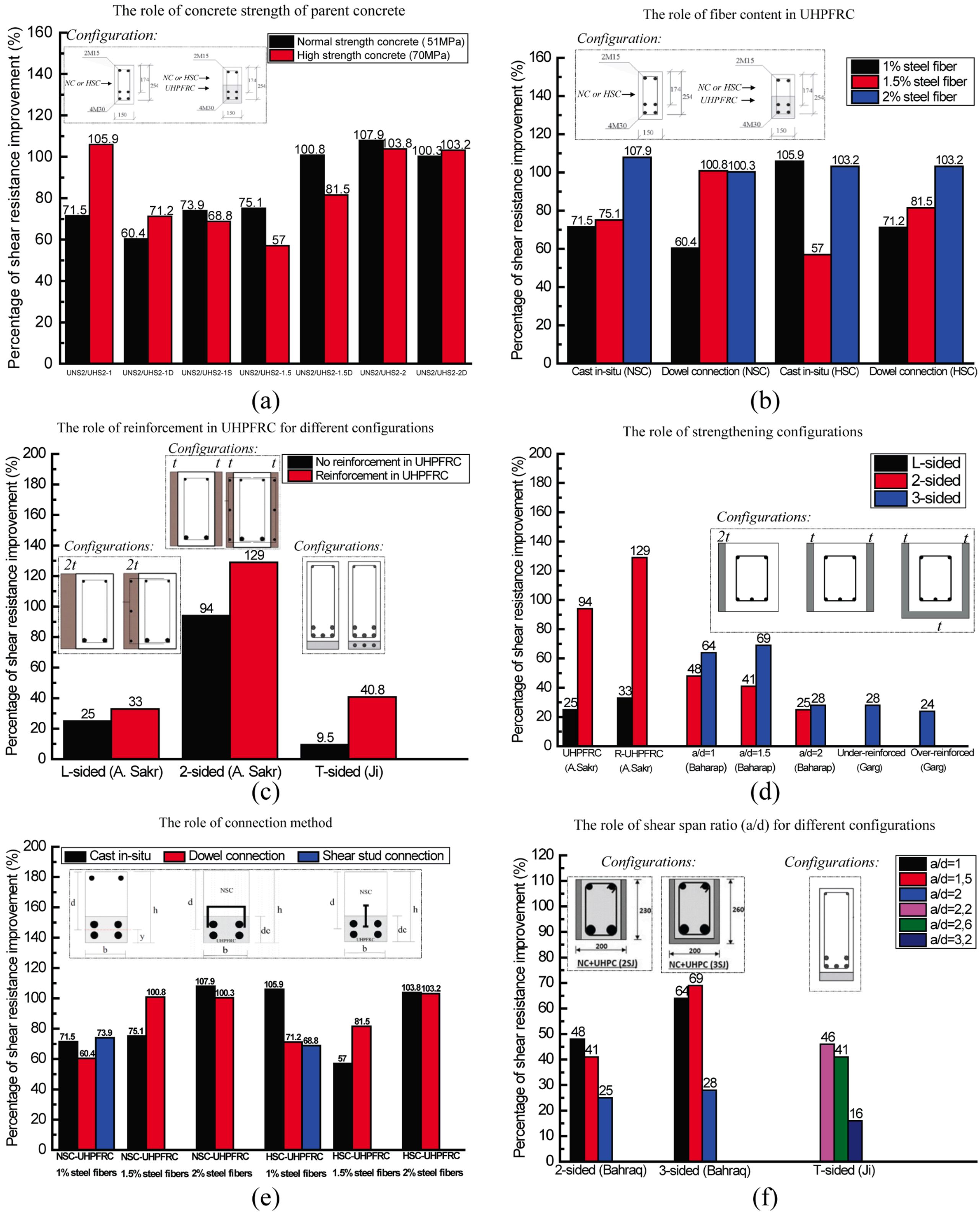

Fig. 4. Parametric analysis for shear strengthening with UHPFRC and percentage of shear resistance improvement with changing: (**a**) concrete strength of parent concrete [47]; (**b**) steel fiber content in UHPFRC [47]; (**c**) reinforcement in UHPFRC [29,30]; (**d**) strengthening configuration [27-29]; (**e**) connection method [24]; (**f**) shear-span ratio (a/d). In Fig. 4a, for the specimen name, the first and second letters indicate two types of concrete to form hybrid specimen followed by the number of specimen configurations, the last number indicates the volume of fiber in UHPFRC and the last letter indicates the connection method. Note that the failure pattern may change after strengthening with UHPFRC, thus the improvement ratio indicated in the figure means the minimum improvement of shear resistance; the negative number shown in (**d**) means the reduction of resistance in 2-sided strengthening pattern due to the debonding failure.

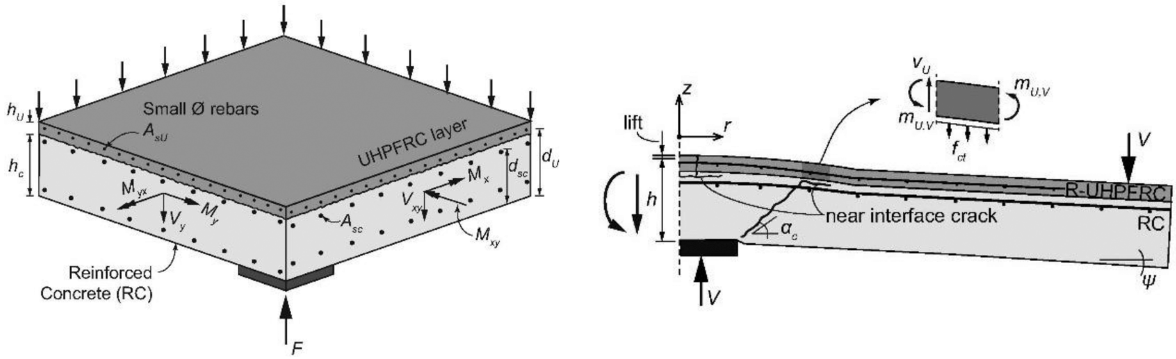

(a) Composite R-UHPFRC-RC slab element (b) Punching shear resistance mechanism

Fig. 5. Punching shear resistance strengthening mechanism with UHPFRC [56].

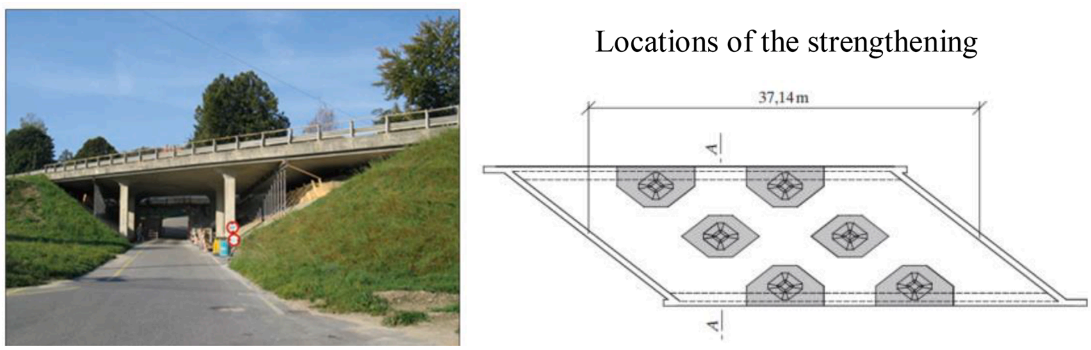

Fig. 6. Slab bridge strengthened with R-UHPFRC over piers (dark areas) in the Switzerland [60].

UHPFRC–RC composite slabs, Masse [58,70] combined global force-rotation behavior derived from analytical composite model and composite failure criterion. This model was upgraded by considering the contribution of the RC compression section to the punching resistance. A unified strength theory-based punching shear strength model for RC slab strengthened with UHPFRC was proposed by Wu et al. [59]. The effects of UHPFRC overlay thickness and tensile strength on the punching shear strength were identified by using the proposed model, and subsequently validated by experiments and numerical study. Similarly as for shear resistance, aforementioned models use the principle of superposition of RC and UHPFRC contribution to calculate the punching shear strength.

The comparison of the predictions with the theoretical model and test results is presented in Fig. 7. All these three models reasonably evaluated the punching shear resistance of hybrid concrete slabs with UHPFRC overlay, although Wu [59] slightly underestimate the measured resistance.

3.2. Numerical modeling of shear and punching shear resistance

Apart from analytical models, numerical analysis is also used to understand and predict the structural behavior of UHPFRC-NC composite structures. However, as mentioned in Section 2.2, until now only few experimental studies focused on the shear performance of RC structures strengthened with UHPFRC, not to mention the lack of valid and reliable numerical methods in this respect. In addition, due to the complexities of shear resistance mechanism such as diversity of contribution from different components, as well as complicated stress state and high nonlinear properties for shear crack, a proper simulation for shear behavior of RC structures is difficult to reproduce [72]. Moreover, material constitutive models of UHPFRC always need to be calibrated due to different fiber contents, geometry and orientation [73]. Finally, the unclear interaction between the steel fibers and the matrix of UHPFRC makes it hard to predict the shear strength improvement [74].

From Table 2, the limited comparison between simulated and experimentally obtained capacities indicates that applied numerical approach is able to predict the shear resistance of UHPFRC-NC hybrid structure although its reliability still needs to be examined and confirmed by enough experimental studies. In line with this, it is not clear if these models can be generically applied for any type of composite structure and boundary conditions.

Typically, the “concrete damage plasticity model” (CDP) is used in UHPFRC hybrid concrete structures to model the nonlinear constitutive behavior of concrete. In CDP, failure modes include concrete tensile cracking and compressive crushing. For UHPFRC, the CDP model is applied [75] but both strain hardening and softening stages from the tensile response of UHPFRC should be included, as shown in Fig. 8. In order to properly predict the shear response of UHPFRC-NC structures, besides the material modeling (of concrete, reinforcement and UHPFRC), attention should be paid to the modeling of the interface between UHPFRC and concrete. So far, usually the perfect bond was assumed [45,50,76,77] since the interface is strong enough to resist the debonding between UHPFRC and NC based on both experimental observation from structural tests and evaluation from bond strength tests if the interface is properly prepared. Instead of adopting perfect bond assumption, some researchers [52,63,75] started considering interface modelling. The cohesive zone model allows slip and debonding by which the interface behavior between concrete and UHPFRC can be described [52,75]. In this model, three parts, namely the linear elastic traction-separation part, the damage initiation point, and the damage evolution zone, are used to describe the damage process (Fig. 9). In simulated hybrid structures, debonding failure mode was well captured only when input parameters including interface shear strength, fracture energy, and elastic shear stiffness are well defined. Besides this model, equivalent beam elements method to simulate the interfacial bond

Table 2
Comparison between analytical or numerical and experimental results.

Reference	Specimen name	Analytical models $V_{u,ana}/V_{u,exp}$	FE studies $V_{u,FE}/V_{u,exp}$
Hussein et al. [47]	NS1	0.45	–
	UNS3-1	0.67	–
	UNS3-1.5	0.82	–
	UNS3-2	0.86	–
	HS1	0.46	–
	UHS3-1	0.70	–
	UHS3-1.5	0.91	–
	UHS3-2	0.85	–
Yin et al. [61,63]	RE-0	0.65	1.05
	OV-25	0.85	0.97
	OV-25a	0.85	1.05
	OV-50	0.94	1.06
	OV-50a	0.80	1.00
	RE-20	0.92	1.05
	RE-32	1.14	0.98
	RE-50	0.8	0.94
	RE-100	1.64	0.97
A. Sakr et al. [52]	C-S	–	0.97
	C-F	–	1.00
	C-S-210	–	1.07
	ST-2S	–	0.96
	ST-1S	–	0.99
	ST-2S-R	–	0.98
	ST-1S-R	–	0.98
Ji et al. [53]	RC-2.7	0.93	–
	RC-U-2.7	0.94	–
	RC-RU-2.7	0.95	–
	RC-RU-2.4	0.96	–
	RC-RU-3.1	0.96	–
Bahraq et al. [50]	CT-1.0	–	0.97
	SB-2SJ-1.0	–	0.96
	SB-3SJ-1.0	–	0.97
	CT-1.5	–	1.03
	SB-2SJ-1.5	–	1.01
	SB-3SJ-1.5	–	1.01
	CT-2.0	–	0.98
	SB-2SJ-2.0	–	1.02
	SB-3SJ-2.0	–	0.97

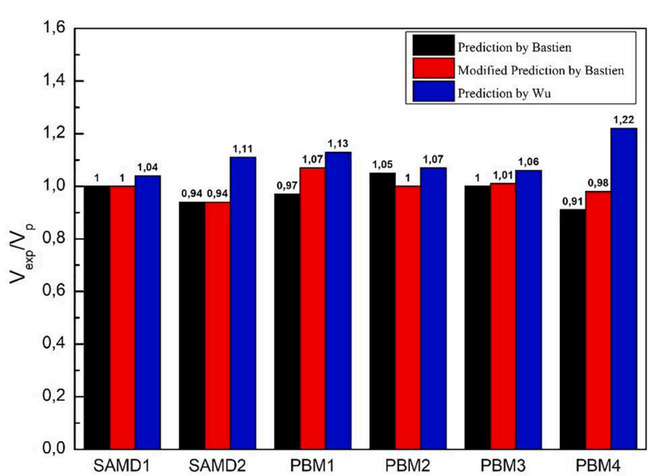

Fig. 7. Comparison of punching shear strength between experimental and predicted results [56,58,59]. (Note: V_{exp}/V_p indicates the ratio between experimental and predicted results, and the series of SAMD samples were tested by Wuest [71], and the series of PBM sample were tested by Bastien [56].).

behavior for UHPFRC–concrete members were proposed by Yin and Shirai [63]. The simulated results obtained by the equivalent beam elements method were reported to have better correlation with experimental results compared to simulation results by using perfect bond or fully unbonded interface.

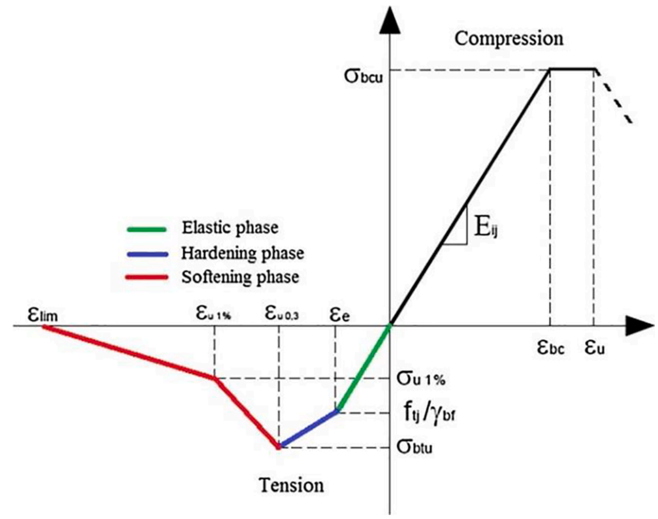

Fig. 8. The uniaxial stress-strain curve for UHPFRC [75].

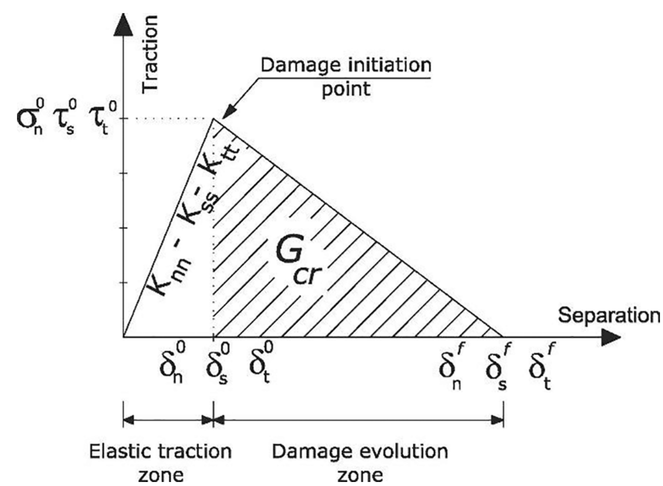

Fig. 9. Bilinear traction-separation law at near interface concrete zone [75].

In practical strengthening applications with UHPFRC, one important quality control of composite UHPFRC-RC elements is that the interface bond strength has to be higher than the tensile strength of the concrete substrate, which is the usual result from in-situ quality control (pull-out) tests. This implies the weakest zone in the strengthened structural system with UHPFRC is the near interface concrete (NIC) zone rather than at the interface, as shown in [56,68]. Failure occurs within NIC zone due to the stiffness change in materials, probably causing stress concentrations near the interface in the concrete part. Consequently, the bilinear traction-separation law shown in Fig. 9 does not apply for the interface between UHPFRC and concrete; however, it is applicable for the concrete fracture in the NIC zone that is determinant. Similar law is used to determine the bond strength of carbon fiber lamellas on concrete substrates where again debonding occurs due to concrete fracture in the zone near the interface as the bond strength of the interface shall always (and can) be made stronger than the tensile strength of the concrete substrate which cannot be increased. Therefore, in order to predict the risk of debonding for concrete structures strengthened with UHPFRC, realistic numerical models to simulate the NIC zone are needed.

4. Behavior of UHPFRC-concrete interfaces in varying bond and structural tests and parameters affecting it

Research [78,79] shows that the interface behavior in the repaired structures is one of the most important factors for structural safety and durability. Though interfacial debonding hardly occurs in practical applications repaired with UHPFRC if surface of the existing concrete substrate is properly prepared and quality control of UHPFRC is provided, a good understanding of interface behavior is still needed to guide interface preparation and minimize the risk of interface failure. In this chapter, interface behavior and the role of governing parameters (type of bond, moisture exchange between the hardening UHPFRC and hardened concrete, etc.) are addressed. Interface behavior is considered through different bond strength tests, but also through structural tests (considering both flexural and shear strengthening applications, especially when delamination is explicitly considered).

Generally there are two types of concrete-to-concrete interfaces – unreinforced and reinforced interfaces [80]. In some applications (e.g. strengthening), having unreinforced interface would ease the execution. For unreinforced interface, interfacial bond strength normally depends on the cohesion (combination of adhesion and aggregate interlock) and friction, which is related to the surface roughness and external force at the interface. For reinforced interface, apart from the abovementioned two parameters, the friction due to clamp effect and dowel action from reinforcement crossing the interface will also contribute to the interface resistance. Environmental and/or mechanical loads will cause stresses at the interface. Compatibility between two materials should be considered because mismatch of material properties (shrinkage, stiffness, strength, coefficient of thermal and hygral expansion) might lead to stress concentrations and interfacial failure [81]. As a rule of thumb, for the purpose of repair and strengthening, new concrete is advised to have similar material characteristics as the original concrete. This is however, not always possible, neither is optimal. Due to different age, it is not possible to have full compatibility between the two concretes in strengthening and repair [82]. Even more, high tensile strength and strain hardening property of UHPFRC, along with low drying shrinkage, are reported to minimize the risks of debonding and excessive cracking [7]. Therefore, it is important to understand systematically the role of time-dependent and coupled mechanical/thermal/hygral processes in hybrid concrete structures.

4.1. Bond strength testing methods to investigate interface behavior

Normally the interface is exposed to a combination of tensile and shear stresses. Tensile stress tends to open the interface crack and shear stress causes sliding along the interface. The interface resistance is governed by the type of interface (reinforced/unreinforced), the properties of substrate (surface preparation, porosity, moisture conditions, strength, etc.), properties of strengthening material, the use of bonding agent [83-85], etc., and it may change due to time-dependent effects [78]. In order to assess resistance of interface under stresses induced by environmental effect and/or mechanical loading, various test methods have been put forward. They can mainly be divided into four categories, depending on the stress condition: tension, pure shear, combination of shear and compressive or tensile stress, and bending test [86]. It is difficult to select a generic test method for evaluating the bond strength in actual structures. It is recommended that the bond test should be selected based on the state of stress that the structure is subjected to in the field [78]. Various researchers [78,87] tried to determine ratios between different bond strength tests. Note that in most of these test methods, usually the failure occurs in the concrete substrate or the strengthening material rather than along the bond plane. Under this condition, the bond strength value and its dependence on governing factors such as surface roughness or bonding agent, are difficult to extract [88]; the measured value presents only the lower bound limit and not the real bond strength.

4.1.1. Tension tests

Tensile bond strength tests can be divided into direct and indirect tensile tests [89-93]. In direct tensile tests, avoiding eccentricity is essential because it will generate additional bending moment and make the test results unreliable [78,94,95]. Compared to direct tensile testing, indirect tension tests such as the splitting test are easier to conduct but are suitable only when the interface is smooth since otherwise, the stress is not uniform along the interface.

The commonly observed failure patterns in UHPFRC-concrete composite elements can be divided into 3 types: (i) failure within the concrete substrate itself (cohesive failure); (ii) failure along the interface (adhesive failure) and (iii) mixed failure both at interface and concrete substrate. Although pull-off and splitting tensile tests are easier to perform and therefore more commonly applied, it was reported that the direct tension test with UHPFRC-concrete enables a higher possibility for interfacial failure to happen [93]. In order to trigger interfacial failure, Valipour et al. [96] modified the pull-off test (Fig. 10 (a)) and proposed a debonding test method (Fig. 10 (b)). Both methods aimed at reducing the contact area between the UHPFRC and the concrete substrate, ensuring that the interface is subjected to high tensile stresses to trigger failure.

4.1.2. Shear tests

Introduced in the context of theory of elasticity of structures, "pure shear" is a theoretical concept but does not exist in reality. In reality, only tension and compression forces/deformations exist in structures. Still many "pure shear" tests for interface, aiming to investigate the state when tension in one direction is equal to compression in perpendicular direction, are developed. Current shear test methods will induce a bending moment due to the eccentricity of the shear force to the interface [97]. Due to this, test methods have been put forward to neutralize the moment as much as possible that the shear force causes but, they could not represent the real condition or are hard to conduct [98]. For concrete-concrete interfaces, shear test methods are divided into torsion shear, Guillotine, push-through, modified vertical shear, bi-surface shear, and direct shear method. Due to the convenience and test stability, bi-surface shear and double-sided shear test methods shown in Fig. 11 have been adopted to investigate the UHPFRC-NC interfacial shear behavior [99,100]. Based on the test results, pure interfacial failure rarely occurs, and mostly occurring is mixed failure and concrete substrate failure. Therefore, new test methods to evaluate the shear bond strength between UHPFRC and concrete are needed.

4.1.3. Shear and tension/compression test

Tests have been conducted to induce combination of shear and tensile/compression stresses in concrete-concrete specimens [97,101]. Slant shear test with a combination of shear and compressive stresses is usually reported to reflect the realistic stress state in composite structures. This test is widely used to investigate the UHPFRC-NC interfacial behavior, as shown in Fig. 12 [89,90,92,93,102]. In common slant shear compressive test, interface is inclined and interfacial failure happens due to the shear crack along the inclined plane. As the angle between the failure plane and the horizontal direction is theoretically between 50–70°, the interface with an angle of 60° is commonly selected. The normal stress σ_n and shear stress τ_n at the interface can be obtained through the following equations.

$$\sigma_n = \frac{P}{A}\cos^2\alpha \tag{6}$$

$$\tau_n = \frac{P}{A}\sin^2\alpha \tag{7}$$

where P is the applied load, A is cross-section area of the specimen, α is the angle between the interface and longitudinal direction.

However, this test method has some shortcomings. Firstly, the standard angle does not always lead to the most critical interfacial stress state since critical bond angles are also related to the surface roughness. The rougher interface will have a lower critical bond angle [84]. Upon increasing the roughness to a certain level, the failure starts to localized

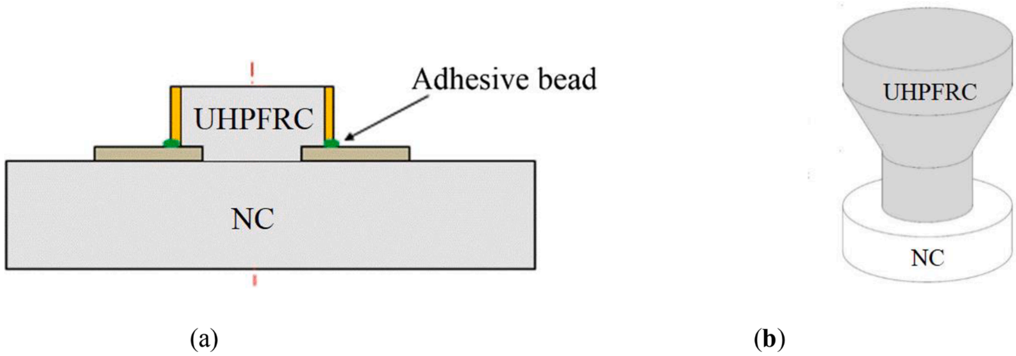

Fig. 10. Test set-up for proposed UHPC debonding test (a) Modified pull-off test (b) Proposed debonding test method [96].

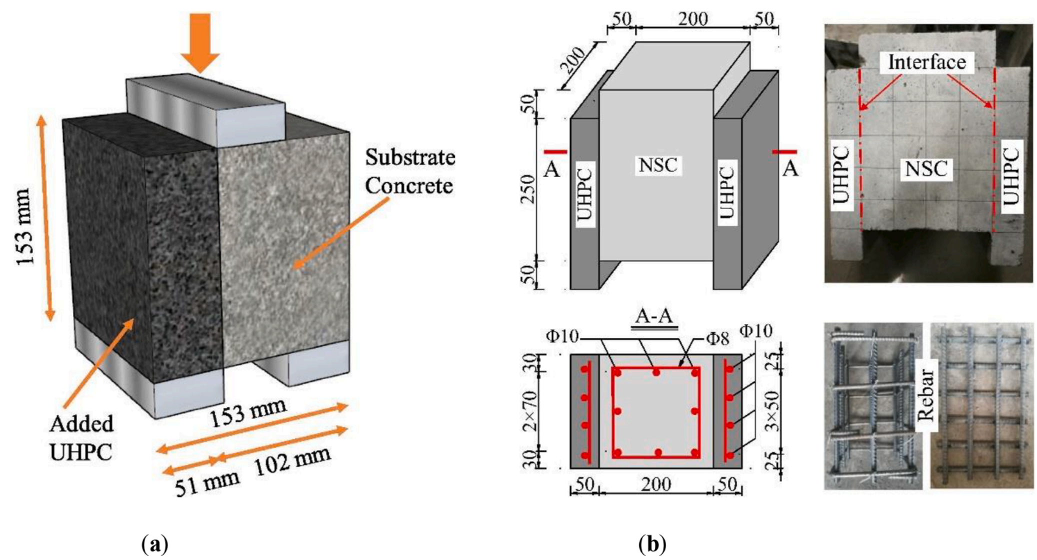

Fig. 11. Shear test: (a) Bi-surface shear [99]; (b) Double-sided shear [100].

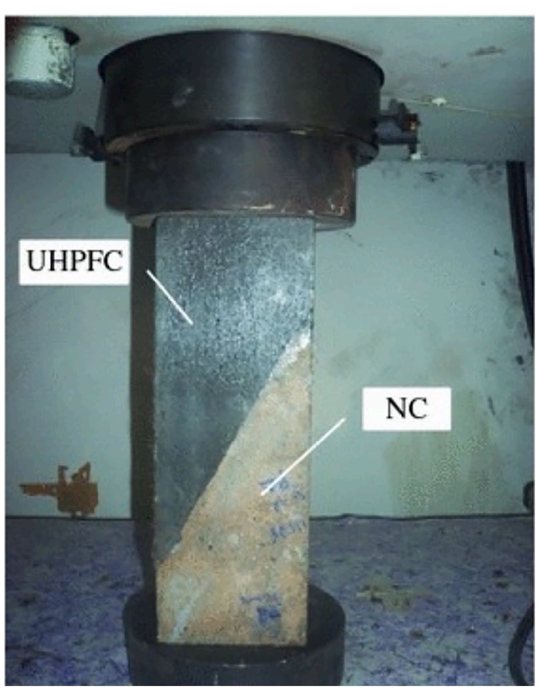

Fig. 12. Slant shear test set-up for UHPFRC-NC specimen [89].

in concrete and the effect of further increase of the roughness at the interface cannot be investigated. Secondly, test results are affected by stress concentrations due to elastic modulus differences of repaired material and substrate [84]. Finally in these tests the pure interfacial failure occurs only under poor interface preparation conditions. As such these tests in most cases are not suitable to determine the real bond strength between UHPFRC and concrete.

4.1.4. Bending tests

Bending tests have also been used for bond characterization between cement-based layers [103,104]. Although the bending test method is reported to represent the actual stress condition of structures and the obtained bond strength is closer to the actual value, it will lead to low efficiency because the area of the bonded surface subjected to loading is small compared to the specimen volume and only a very small part of the bonded plane is subjected to the maximum stresses [78]. Fig. 13 shows the typical set-up to investigate the bond behavior between UHPFRC and NC by four-point bending test. The modulus of rupture is used to evaluate the interface behavior between two different concretes and, when the shear span is 1/3 of the support span, it can be calculated as follows:

$$R = \frac{2Pl}{bd^2} \tag{8}$$

where R is modulus of rupture or flexural strength, P is maximum applied load, L is length of the span, b and d are width and depth of the specimen respectively.

Experimental studies using this method [92,102] showed that typical

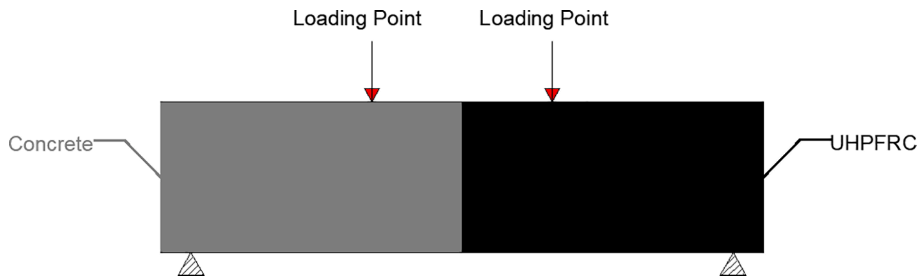

Fig. 13. Four-point bending test.

failure happens either at the interface or in the concrete substrate, with the fully interfacial failure occurring only when the interface is smooth.

4.1.5. Comparison of test methods

In line with above discussion on strengths and weaknesses of different test methods, it can be observed that the (modified) pull-off and slant shear tests are the most commonly applied test methods to study the UHPFRC-NC interface behavior under tensile and shear stresses. However, in general for concrete-to-concrete interfaces (and not only related to UHPFRC-concrete), two main conclusions can be made. Firstly, there is no unified test for concrete-to-concrete interface behaviour. An attempt to determine the relationship between bond strength results from different test methods is made in [105]. Secondly, in commonly applied tests, actual interfacial strength is not measured since the failure usually occurs in the weaker concrete substrate rather than along the interface between UHPFRC and concrete.

4.2. Influence of bonding techniques and roughness profile on bond capacity

Currently, there are three main bonding techniques to strengthen damaged concrete structures with UHPFRC: Cast in-situ, gluing with a bonding agent and mechanical anchoring. Different bonding techniques will lead to different bond strengths. Due to its convenience and simplicity, cast in-situ is the most popular bonding technique for concrete structures strengthened with UHPFRC.

The role of the applied bonding technique in UHPFRC-NC composites on measured bond strength was investigated in [77]. Cast in-situ specimens with smooth surface had the lowest bond strength based on splitting tensile and slant shear tests (Fig. 14). Cast-in situ specimens where concrete was prepared by sandblasting resulted in the highest bond strength in slant shear test. On the other hand, bonding UHPFRC at

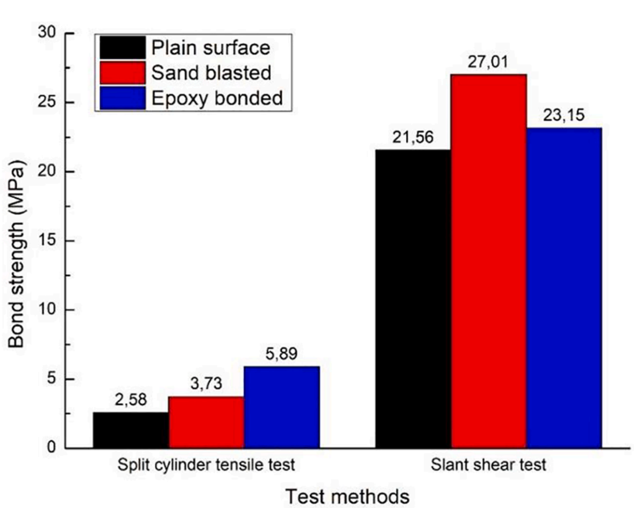

Fig. 14. Bond strength test results [77].

the smooth surface of concrete substrate with epoxy adhesives had the highest bond strength in the splitting tensile test. This was contributed to the mechanisms of adhesion and friction along the interface. In splitting tensile tests, the tensile stress is mainly governing and thus adhesion between concrete substrate and UHPFRC plays a dominant role on the interfacial bond strength. Bonding with epoxy seems to provide a higher splitting tensile strength compared to the other two methods. However, under slant shear testing in which the interface is loaded in combination of compression and shear, sandblasting the concrete substrate improves the roughness of the surface to resist shear stress, and may lead to the highest bond strength among these three methods.

In terms of shear improvement, the comparison of different bonding techniques (cast in-situ and mechanical anchorage through dowel and shear stud connection) on the structural shear capacity is shown in Fig. 8 (e). The results show that the effect of mechanical anchorage is negligible provided that there is no interface failure in reference samples.

Although it is for flexural performance of reinforced concrete beams strengthened with UHPFRC, studies [41,44,77,106,107] which discussed the effect of different bonding techniques: (1) in-situ application of UHPFRC, (2) gluing with UHPFRC laminate and (3) the use of mechanical anchorage, were reviewed. The effectiveness for strengthening by casting UHPFRC in-situ or gluing precast UHPFRC strips with epoxy adhesive was studied by AI-Osta et al. [77]. Tanarslan et al. [107] compared the flexural performance of concrete beams strengthened with UHPFRC by different bonding methods (gluing with epoxy or mechanical anchoring). An overview of the test results and the corresponding strengthening configuration [77,107] is presented in Table 3 and Fig. 15.

In general, for all bonding types, specimens strengthened with UHPFRC improve the bearing capacity while they reduce the deflections (see Fig. 16 and Fig. 17). For all studied bonding techniques there is no significant difference for loading and deflection capacity and no interfacial failure was observed. It seems that under the same strengthening configuration, all bonding techniques do not change the failure mode: beams strengthened by different techniques fail in the same way. It is worth noting that the aforementioned conclusions are drawn based on results of strengthened beams without reinforcement in UHPFRC. However, when rebars are added in UHPFRC, epoxy bonding results in larger capacity increase compared to mechanical anchorage, but the deflection ability of these beams is largely reduced and results in brittle failure. In addition, all bonding techniques greatly enhance the cracking resistance and the efficiency from high to low is gluing with epoxy, cast in-situ and bonding with mechanical anchorage, because the cross-section of UHPFRC is weakened by the anchorage holes and cracking easily occurs and propagates away from these sections (see Fig. 18).

All these studies focused on the flexural performance improvement of RC beams with UHPFRC, whereas studies on shear strengthening with UHPFRC by using different bonding techniques are lacking. Besides mechanical performance, type of bond would also influence the durability. Although experimental results have shown that the impermeability of strengthened concrete beams with UHPFRC is superior and the ingress of air and water by in-situ cast UHPFRC is largely reduced [90], no study assessed the same performance by using epoxy adhesive or

Table 3
Overview of beam test results under flexure [77,107].

Reference	Specimen name	Dimension $b \times h \times L$ (mm)	Strengthening technique	Strengthening pattern		Cracking load (kN)	Failure load (kN)	Deflection at failure load (mm)	Failure type
				Configuration	UHPFRC Thickness				
Al-Osta et al. [77]	RC-control	140×230×1600	–	–	–	16	70	19.10	Flexure
	RC-SB-BOTSJ	140×260×1600	Cast in-situ	T-sided	30 mm	33	81	15.31	Flexure
	RC-EP-BOTSJ	140×260×1600	Gluing by epoxy	T-sided	30 mm	47	75	12.13	Flexure
	RC-SB-2 SJ	200×230×1600	Cast in-situ	2-sided	30 mm	41	102	13.38	Flexure
	RC-EP-2 SJ	200×230×1600	Gluing by epoxy	2-sided	30 mm	44	95	15.7	Flexure
	RC-SB-3 SJ	200×260×1600	Cast in-situ	3-sided	30 mm	90	132	4.55	Flexure
	RC-EP-3 SJ	200×260×1600	Gluing by epoxy	3-sided	30 mm	95	85	4.35	Flexure
Tanarslan et al. [107]	Beam-1	120×160×3200	–	–	–	10.52	41.96	75.53	Flexure
	Beam-2	120×190×3200	Gluing by epoxy	T-sided	30 mm	23.05	48.52	65.22	Flexure
	Beam-3	120×190×3200	Mechanical anchorage	T-sided	30 mm	14.32	46.42	54.16	Flexure
	Beam-4	120×190×3200	Gluing by epoxy	T-sided	30 mm with reinforcement	41.32	94.27	24.66	Concrete cover tearing
	Beam-5	120×190×3200	Mechanical anchorage	T-sided	30 mm with reinforcement	29.94	72.63	71.63	Flexure

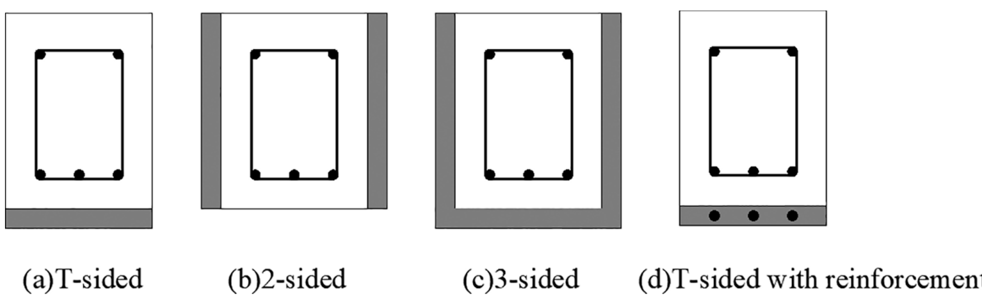

Fig. 15. Strengthening configuration [77,107].

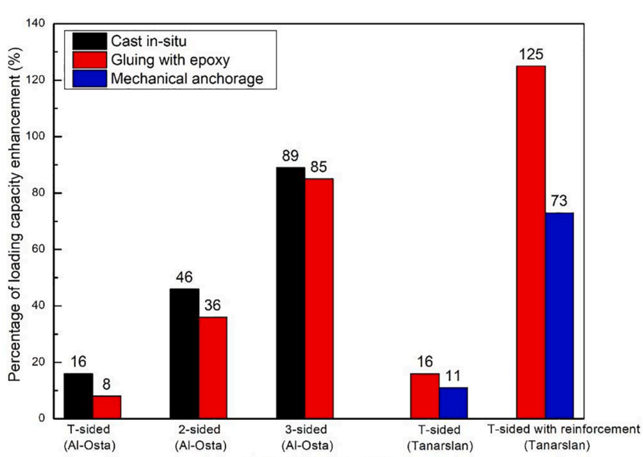

Fig. 16. Loading capacity enhancement with different bonding techniques (calculated as $(F_{u,s}/F_{u,c} - 1) \times 100\%$, $F_{u,s}$ is peak load of strengthened beam, $F_{u,c}$ is peak load of control beam) [77,107].

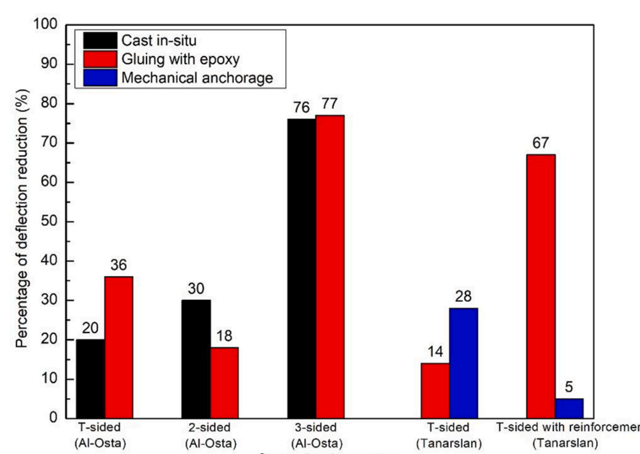

Fig. 17. Deflection reduction with different bonding techniques (calculated as $(1 - \Delta_s/\Delta_c) \times 100\%$, Δ_s is displacement at peak load of strengthened beam, Δ_c is displacement at peak load of control beam) [77,107].

anchoring.

4.3. Influence of moisture exchange on interface behavior

Although being relevant only for cast in-situ applications, moisture exchange is addressed as well. Restrained shrinkage stress and possible cracking/delamination are closely related to microclimatic state of the substrate (moisture and thermal conditions) and on-site environmental conditions [108]. Firstly, the moisture exchange between the strengthening material and the concrete substrate will affect the cement hydration and therefore determine the interface quality and the interface bond strength [109-111]. Although it is reported to detrimentally affect the microstructure and the interfacial bond strength [112,113], and increase the air content at the vicinity of the interface [82], on the other side, moisture transport is also reported to improve mechanical anchorage between the two materials [87]. Secondly the moisture exchange cause moisture gradients resulting in differential shrinkage and stress concentrations at the interface. The moisture exchange depends

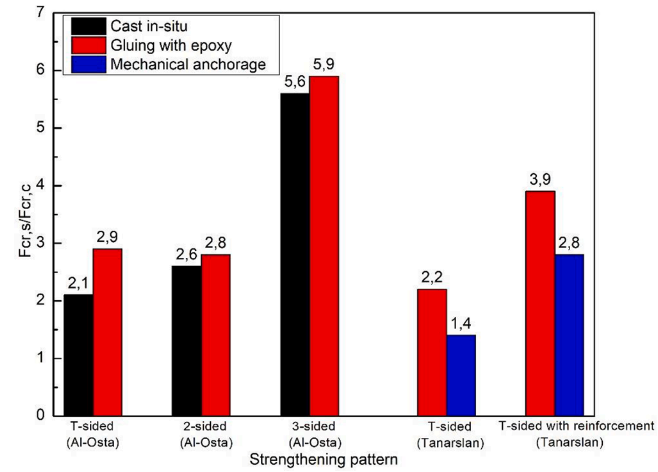

Fig. 18. Cracking resistance improvement with different bonding techniques (denoted as$F_{cr,s}/F_{cr,c}$,$F_{cr,s}$ is initial cracking load of strengthened beam, $F_{cr,c}$ is initial cracking load of control beam) [77,107].

on the water content and the porosity in the concrete substrate, hydration rate and transport properties of UHPFRC, and drying conditions in the environment.

Moisture exchange can have different effect on different types of bond resistance. A recent study on normal strength concrete interface [87] shows that with regard to the tensile bond strength, the Saturated Surface Dry (SSD) condition increases the hydration of the strengthening material and consolidates the strengthening material to create a denser interface. With regard to the shear bond strength, SSD condition produced lower bond strength compared to a dry, roughened substrate. It was explained that particles in the strengthening material will be drawn into the surface profile of a roughed substrate, creating more solid-solid contacts which are useful to generate friction along the interface.

Fresh UHPFRC does not behave in the same way as fresh concrete (which has an excess of water with respect to the cement content). Compared to the strengthening material with a w/c ratio of more than 0.3 [87,112,113], the moisture state of substrate and environmental conditions probably has a greater impact on UHPFRC (i.e. w/c ratio less than 0.25). For UHPFRC, in terms of rapid drying of exposed surface due to fast water evaporation to surrounding environment, absorption by concrete substrate and self desiccation of UHPFRC, the curing methods have a great impact on the quality of UHPFRC [114]. Moreover, although the rate of moisture exchange from UHPFRC to the substrate is lower compared to normal or high strength concrete [115], due to its low w/c ratio and the fact that the rate of moisture loss from the freshly cast cement to dry substrate is the same as absorption rate of free water [116], the moisture exchange might be detrimental, especially when a thin layer of UHPFRC is cast. Therefore, as a rule of thumb, for on-site applications with fresh UHPFRC, in order to have a high bond strength at the interface, the existing concrete substrate should be moist wet with a dry surface prior to casting fresh UHPFRC. Fig. 19 shows that in both tension and shear bond strength tests, for the three tested moisture conditions of the substrate, SSD is the optimal condition to get a higher bond strength for UHPFRC [117], which is contradictory to the finding for shear bond strength obtained for normal strength concrete in [87]. More systematic approach to investigate the role of moisture exchange in UHPFRC-NC composite is needed. The effect of thickness ratio between UHPFRC and substrate, the optimal moisture state of substrate and curing conditions of strengthened system should be investigated.

4.4. Influence of shrinkage on interface behavior

When the hybrid structure is subjected to drying shrinkage, restrains due to the connection of overlay and substrate results in tensile stress in the drying material and debonding stresses at interface (Fig. 20), which may cause debonding and failure of the interface [118]. In this context, acting as an internal load, shrinkage is one of the most important parameters influencing the performance of a strengthened concrete structure.

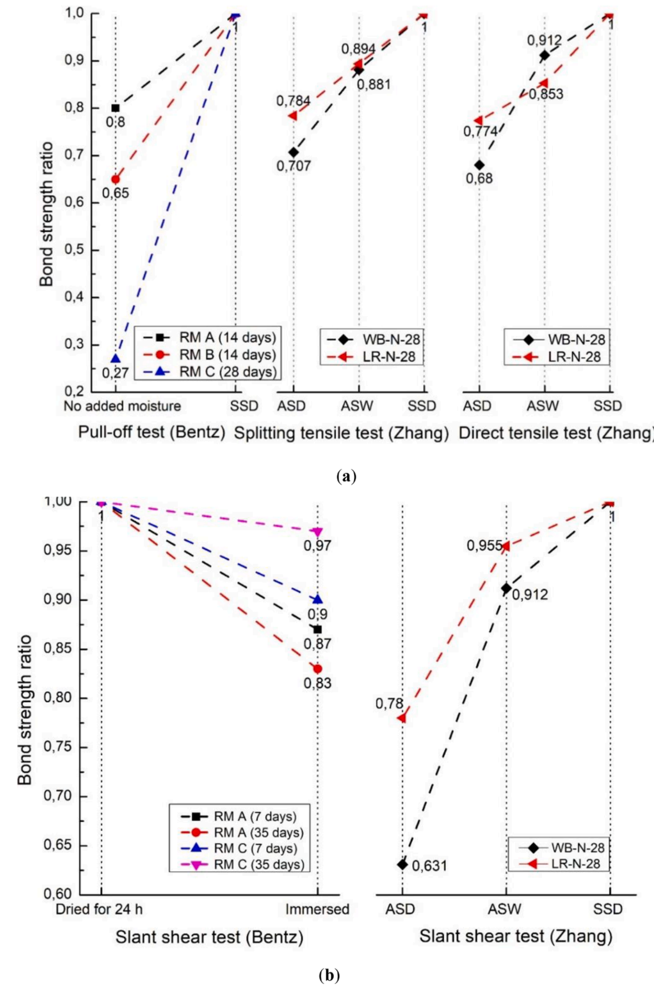

Fig. 19. Effects of moisture state of substrate on relative bond strength for different repair materials (named RM A, RM B and RM C, WB-N-28 and LR-N-28) and different moisture state of substrate (SSD, ASD and ASW stand for saturated surface dry conditions, air surface dry condition and air surface wet condition respectively.): (a) Effects of moisture state of substrate on tensile bond strength for normal strength concrete (RM A, RM B and RM C) and UHPFRC (WB-N-28 and LR-N-28); (b) Effects of moisture state of substrate on shear bond strength for normal strength concrete (RM A, RM B and RM C) and UHPFRC (WB-N-28 and LR-N-28) [87,117].

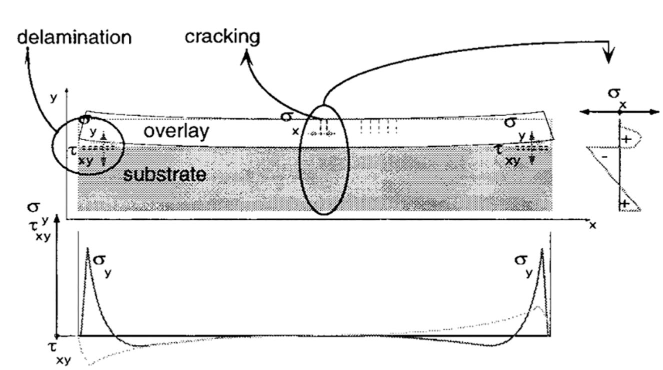

Fig. 20. Damage mechanisms in strengthening systems [82,118].

In UHPFRC drying shrinkage is small (<200 μm/m) but the autogenous shrinkage (>400 μm/m) is dominant [108,119-123]. For strengthening applications of in-situ cast UHPFRC without thermal curing, internal restrained stress caused by autogenous shrinkage should be considered in the strengthening design stage. Restrained shrinkage of concrete structures strengthened with UHPFRC has been studied experimentally [124,125]. It was concluded that autogenous shrinkage is important in the first 90 days after casting the UHPFRC layers and the shrinkage-induced tensile stress increases as the fiber content and thickness of UHPFRC decrease (Fig. 21). In addition, tests have also been conducted to study the restrained shrinkage stress of reinforced UHPFRC and reinforced UHPFRC-RC composites under normal curing and steam curing. Strain gauges were attached close to the interface both in RC and UHPFRC layers to measure the strain and to calculate interfacial stress between reinforced UHPFRC and reinforced concrete. Note that these calculations, however, are extremely difficult to be performed, due to different influencing parameters (e.g. time-dependent creep of substrate, relaxation of UHPFRC, amount of restraint at the interface, etc.). Compared to normal curing, steam curing does not affect the measured shrinkage. On the other hand reinforcement inside the UHPFRC and concrete substrate reduce the measured shrinkage [126] (Fig. 22).

Due to the high tensile strength and strain hardening property of UHPFRC, it is reported [127] that debonding is unlikely to occur at the UHPFRC-NC interface. However, in some specific circumstances, such as poor substrate preparation, harsh climate on site and inadequate connection between the overlay and the substrate, tensile strength and deformability of UHPFRC are compromised [108]. Under such severe conditions, combined with the mechanical loading, it is still unclear whether the restrained stress will overcome the bond strength.

4.5. *Durability of concrete structures strengthened with UHPFRC*

Durability of the repaired material and the life-cycle cost of the repaired system are two main factors to determine the quality of the strengthened structure [24,128]. The high impermeability of UHPFRC can be a critical property for repair and strengthening in severe environmental conditions.

Experiments including water capillary absorption test [11,129], air/gas permeability test [130] and durability tests [131] (freeze-thaw, chloride penetration, etc.) confirmed the outstanding protective properties of UHPFRC. Due to the excellent durability of UHPFRC, it has been used as a protective layer to prevent the detrimental effect of exposure to aggressive environment. Guingot et al. [132] performed several rehabilitation projects where structures such as dams and bridge channels should be protected from water impact, abrasion and extreme environmental condition. Denairé et al. [133] proposed a method to apply in-situ cast UHPFRC to protect a lighthouse in an aggressive marine environment.

Tayeh et al. [90] evaluated the permeability of the interface between the NC substrate and UHPFRC by means of the rapid chloride permeability, gas and water permeability tests. The test results showed that the interfacial quality can resist the penetration of chlorides as well as significantly reduce the gas and water permeation, validated by the microscopic observations at the interfacial transition zone. Muñoz [127] carried out splitting tensile tests with different numbers of freeze-thaw cycles to evaluate the bond performance of UHPFRC-NC composites in severe environmental conditions. Results shown in Fig. 23 indicate that a greater bond strength is obtained as the number of cycles increases due to hydration of unhydrated cement particles at the interface in the presence of water.

Though the superior durability of UHPFRC-NC composites has partly been validated through small scale splitting tensile tests, the deeper multiscale (macro- meso- and microstructural) analysis of the interfacial zone and interface behaviour is still lacking.

4.6. *Debonding and slip at the interface in structural tests*

Experimental investigations focused on the flexural behavior of composite UHPFRC-NC elements showed that no debonding was observed in the interface zone and the beams behaved monolithically before reaching to maximum resistance [36,44-47]. With UHPFRC-NC specimens, bond strength tests including the pull-out tests, indirect tensile and slant shear tests were carried out and the results showed that the bond strength between UHPFRC and NC is greater than the tensile strength of NC [90,127]. Therefore, the interfacial slip was negligible and was not considered. Hence, perfect bond and monolithic behavior of the composite beam are considered both in numerical modelling and theoretical calculation, and various theoretical calculation models based on this assumption have been put forward [48,59,68,77]. However, based on the "perfect bond" assumption, though the numerical results for structural load-deflection response are accurate, the unsatisfactory predicted crack pattern implies the weakness of this assumption [134]. Moreover, it cannot be generalized that RC structures strengthened with UHPFRC are unlikely to fail due to interfacial debonding. As shown in Fig. 24, the interfacial debonding may still happen with the application of UHPFRC [52,107]. Unlike state-of-art practice for strengthening applications, in which fresh UHPFRC should be cast on-site on previously wet concrete substrate, in both [52] and [107], the epoxy-bonded technique is used to bond the UHPFRC prefabricated laminate and concrete substrate.

It is reported [41] that compared to the interface slip value between two conventional concretes, the value of slip for UHPFRC to conventional concrete interface is significantly lower because UHPFRC with steel fibers has a higher bond strength. In [88], for fiber reinforced

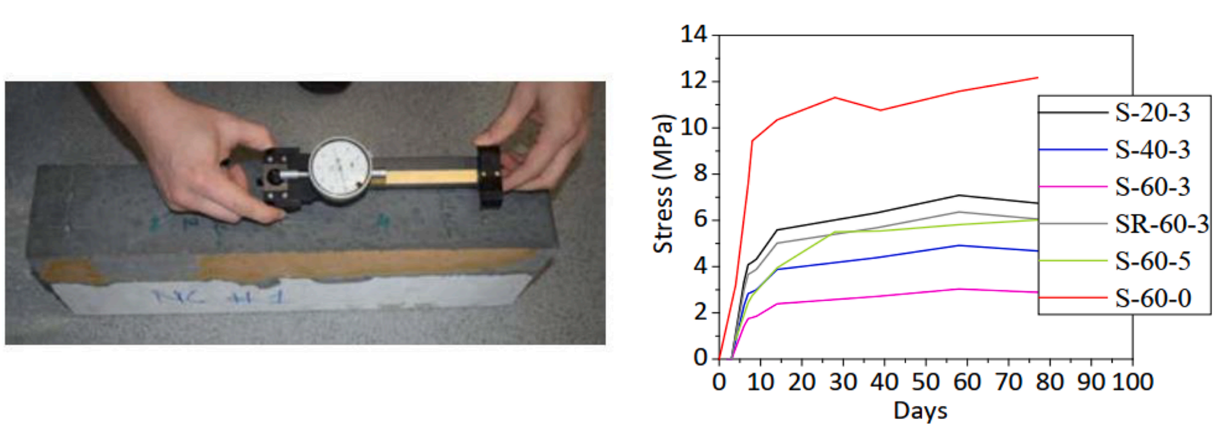

Fig. 21. Restrained concrete shrinkage stresses (S and SR respectively denote strengthened UHPFRC with or without rebars inserted in UHPFRC layer, 20, 40, 60 denote the thickness of UHPFRC layer in mm and 0, 3, 5 denote the volume percentage content of steel fiber.) [124].

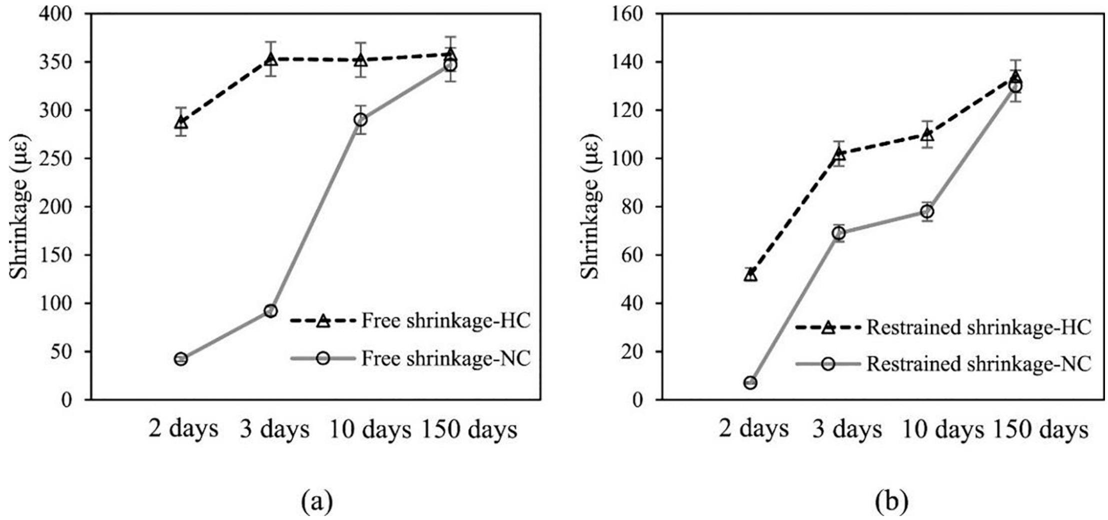

Fig. 22. Free and restrained shrinkage in (a) reinforced UHPFRC and (b) reinforced UHPFRC-concrete composite under different curing conditions (NC and HC respectively denote normal curing and steam curing condition) [126].

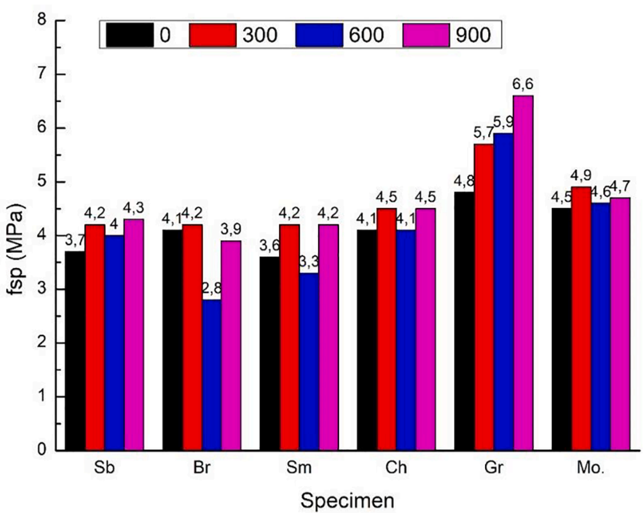

Fig. 23. Effect of freeze–thaw cycles on splitting tensile strength of composite specimen (f_{sp}=splitting tensile stress, Sb = sandblasted; Br = Brushed; Sm = smooth; Ch = chipped; Gr = grooved; Mo = monolithic (only concrete)) [127].

concrete with poly-vinyl-alcohol (PVA) fibers, it was explained that fibers prevent the bond failure as they increase the cohesion at the interface thus reduce the damage due to shrinkage, leading to a higher bond strength value. Another potential reason is the reduction of bleeding at the interface due to fiber reinforcement. However, that does not mean that interfacial slip will not affect the structural performance of composite structures in different strengthening configurations [135]. Moreover, design code "Structural Connections for Precast Concrete Buildings" [136] sets strict slip allowance values, specifically, not exceed 0.2 mm and 2 mm at service stage and in the ultimate state respectively. Paschalis [41] measured the interfacial slip and the maximum slip exceeding 0.3 mm, although bonding between UHPFRC and NC was still effective since the interface is reinforced by the connection steel bars. Tsioulou [104] found that interface preparation and strengthening type: (1) tensile (UHPFRC along whole tensile zone), (2) partly tensile (UHPFRC along central tensile zone) and (3) compressive (UHPFRC along whole compressive zone) strengthening affects the strengthening efficiency. Test results showed that for rough interface, the tensile strengthening type greatly improved the loading capacity while partly tensile strengthening showed the worst performance due to the debonding between UHPFRC and concrete layers. Even more, partly tensile strengthening will lead to a maximum slip value (almost 9 mm) resulted from only mechanical loading (i.e. without including the measurement of initial slip at the interface due to

Fig. 24. Debonding at the interface [52,107].

restrained shrinkage).

Restrained shrinkage also plays a role and might cause slip or debonding, as mentioned in section 4.4. With the additional initial shrinkage strain, FEM analyses have been conducted and the results presented in Fig. 25 show that the slip value along the interface at the ultimate resistance is the lowest for specimen strengthened with three-side jacketing while the specimen strengthened at the tensile side had the highest slip value [135]. Due to the importance of interface property, numerical studies for the strengthened concrete structure with UHPFRC start to consider the interface modelling technique. In [41], based on the push-off bond strength test results, parameters including the friction coefficient and cohesion are calculated through Mohr-column equation in Eurocode 2 [65]. With the above obtained parameters, two dimensional contact element is used to describe the interface property and results show a good agreement between the numerical and the experimental results for the strengthened beam with UHPFRC. In addition, Zhu et al. [137] applied two different interface modelling techniques, namely adhesion and friction based on AASHTO [138] and friction only based on ACI [139] to simulate performances of damaged concrete slabs strengthened with UHPFRC. Results show that compared to the interface model in ACI concept, FE modelling with AASHTO interface concepts is more effective in terms of load-displacement response prediction. Since the interface properties both affect the structural capacity and failure mode, it seems that modified analytical and FEM models with suitable interface modelling that can accurately predict the resistance of the composite need to be put forward. They should contribute to a better understanding of the interface behavior on the composite structural performance, evaluation of debonding risk and optimization of the strengthening method with UHPFRC.

Generally, resistance of UHPFRC-NC bond, under flexural, shear, punching shear and torsional loading, has been studied extensively [36,38,40,41,44-46,57,59,68,77,107,140-143]. However, most tests are focused on the behavior of strengthened beams under mechanical loading and under controlled laboratory conditions, and there is a lack of information related to the combined environmental (exposure to drying, different deterioration mechanisms and aging) and mechanical loads. These combined loadings, presenting better practical conditions, might cause gradients (temperature, moisture, stress, etc.) and stress concentrations at the interface, possibly leading to premature debonding and slip.

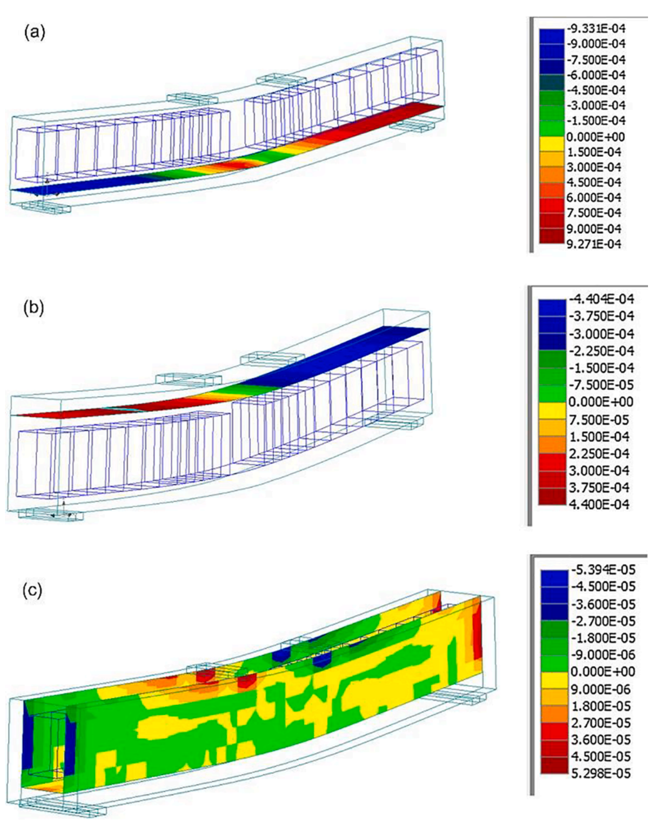

Fig. 25. Interface slip (m) for strengthened beams at ultimate resistance with different UHPFRC configuration: (a) the tensile side, (b) the compressive side, and (c) three sides jacket [135].

5. Conclusions

This paper reviews the state-of-the-art on the performance of concrete structures strengthened with UHPFRC, focusing on shear strengthening. Note that in this overview, not only strengthening applications, but also applications of UHPFRC in new hybrid structures, where the shear capacity improvement was tested, are considered. Many aspects were discussed, starting from structural behavior at the macro-scale, available numerical and analytical methods, through the interface behavior at the meso-scale and its governing parameters. The following conclusions can be drawn:

(1) Most experimental studies showed that for flexural strengthening of concrete structures with UHPFRC, the composite structure almost always behaves monolithically, without debonding and with a limited slip at the interface. Note that, however, all studies considered only mechanical loading of the samples cured in laboratory conditions. No study on structural scale combining mechanical and environmental loads (dry-wet or freeze-thaw cycles), which resembles more practical conditions, has been performed.

(2) For shear strengthening applications of UHPFRC, the effect of concrete strength, steel fiber and reinforcement in UHPFRC, strengthening configuration, connection method and shear span ratio have been investigated. It can be concluded that the concrete compressive strength and the connection method have negligible effect on the shear performance of the composite structure provided that the interface does not fail. The shear capacity improvement increases when reinforcement is positioned in the UHPFRC layer or when the shear span ratio reduces. Moreover, the 2-sided strengthening configuration, although not optimal for durability reasons, seems to be the optimal method for mechanical resistance. The effect of fiber content is still unclear in view of shear capacity of composite beams.

(3) Numerous analytical methods have been proposed in literature. For flexural resistance calculations of UHPFRC-NC composite structures, the assumptions of plain section and perfect bond between the UHPFRC and RC are usually applied for flexural design. For shear capacity calculations, mainly two methods can be classified: one proposes that the shear resistance is always simplified as the sum of the contributions of concrete, the stirrups and the R-UHPFRC element, and the other method involves the additional shear resistance provided by the fibers. Similar to the shear resistance calculation, the punching shear resistance of the composite structure is in the form of superposition of the contributions of concrete and the UHPFRC layer. Results obtained by analytical models for shear resistance of UHPFRC-NC composite structure deviate largely from experimental observations.

(4) Bond strength tests including pull-off and slant shear tests are usually selected to study the bond behavior between UHPFRC and concrete. The pure bond failure occurs mostly in smooth interfaces while the concrete substrate failure and mixed failure are the mostly occurring failure modes for rougher surfaces. In general, the measured bond strength varies greatly dependent on the bond strength test method, there is no unified bond test, and the real interface strength is usually not measured as the

interfacial bond strength for RC structures strengthened with UHPFRC is usually larger than the strength of concrete substrate.

(5) Three main bonding techniques are usually applied to strengthen the existing concrete structures with UHPFRC, namely (1) cast in-situ, (2) gluing and (3) mechanical anchorage. In terms of loading capacity enhancement and deformations in flexural tests (i.e. only mechanical loading), all of them are effective and show an overall good performance provided there exists no interfacial failure.

(6) For cast in-situ application with UHPFRC, the moisture exchange between UHPFRC and concrete as well as water loss from the exposed surface plays a great role. Based on limited current studies, it can be observed that the rate of moisture exchange in UHPFRC composite is lower than that for normal concrete-concrete composite, although due to lower w/c ratio, the effect might be higher. In addition, a proper curing method is of great importance to prevent moisture from transferring to surrounding environment.

(7) Due to a low water-cement ratio of UHPFRC, autogenous shrinkage accounts for the majority of total shrinkage and it significantly increases during the first 90 days. For cast in-situ applications, internal tensile stress at the interface occurs owing to the restraint shrinkage due to the bond with the concrete substrate, and it is reported to increase as the content of steel fibers and the layer's thickness reduce. In general, the strain hardening property and high tensile strength of UHPFRC ensure the monolithic action between UHPFRC and concrete, and thus no crack or debonding were reported at the interface.

(8) The dense structure of UHPFRC enables superior durability. Therefore, it is advantageous for concrete structures rehabilitated with UHPFRC to resist aggressive environments such as freeze-thaw, chloride ingression and water/gas permeation. Moreover, the durability of interface has been examined by capillary absorption, air/gas permeability and other durability tests (freeze-thaw, chloride penetration); results show that the interfacial bond quality is high enough to resist severe environmental conditions.

(9) There has been very limited or no study on combined mechanical and environmental loads including coupled mechanical-hygro-thermal processes in the strengthening system.

6. Recommendations for further research

In order to better understand the mechanical performance of concrete structures rehabilitated with UHPFRC, further researches are recommended to conduct as follows:

(1) Flexural improvement of existing RC structures strengthened with UHPFRC has been sufficiently investigated in experimental investigations and numerical analyses. However, knowledge on shear-deficient RC structures strengthened with UHPFRC is lacking.

(2) Different bond strength values can be obtained with different bond strength tests and the interface failure is usually not observed with UHPFRC-NC composite specimens. The challenge is to develop, preferably simple, bond strength test where the failure would be triggered to happen at interface itself.

(3) For cast in-situ strengthening applications, moisture exchange between UHPFRC and concrete is critical for the microstructure development of UHPFRC. Multiscale approach is needed to systematically study the influence of moisture transport on the bond quality and microstructure of the repair or strengthening system.

(4) For cast in-situ strengthening applications, interfacial tensile stresses induced by restrained shrinkage of UHPFRC pose a threat with debonding/slip at the interface as a potential consequence. While most of studies have shown that the bond is good enough to resist shrinkage stresses, for the combination of restrained stress with action of mechanical loading, it is still unclear what the risk of debonding is. Similarly, the durability of interface is of great importance to guarantee the long service life of UHPFRC-NC strengthened systems. Analysis of the interface behavior under combination of severe environmental conditions and mechanical loading should be identified.

(5) Based on the experimental observations (in the constant lab conditions) that a strengthened structure behaves almost monolithically, perfect bond is generally assumed at the interface. New analytical and finite element approaches should be developed to better understand and predict the actual interface behavior.

(6) Pilot tests on a real bridge strengthened with UHPFRC in shear, typically focusing on the interface preparation prior to the application of UHPFRC, are suggested to conduct for further investigation and on-site application.

Declaration of Competing Interest

The authors declare that they have no known competing financial interests or personal relationships that could have appeared to influence the work reported in this paper.

Acknowledgment

This work was supported by the Dutch Organization for Scientific Research (NWO) under the grant "Optimization of interface behaviour for innovative hybrid concrete structures" (project number 16814). Yitao Huang would like to acknowledge the funding support from China Scholarship Council (CSC) under the grant CSC No. 201906950087. The APC was funded by Delft University of Technology Library.

References

[1] El Kechebour, B.; Zeloum, H. Choice between Retrofitting and Reconstruction of Buildings in Reinforced Concrete after an Earthquake. In Adv. Mater. Res., 2015; Trans Tech Publ.

[2] Brühwiler, E. Rehabilitation of concrete bridges using Ultra-High Performance Fibre Reinforced Concrete (UHPFRC). In Life-Cycle and Sustainability of Civil Infrastructure Systems: Proceedings of the Third International Symposium on Life-Cycle Civil Engineering (IALCCE'12), Vienna, Austria, 2012.

[3] A.E. Naaman, K. Wille, The path to ultra-high performance fiber reinforced concrete (UHP-FRC): five decades of progress, In Proceedings of Hipermat (2012).

[4] A.M. Matos, S.C. Figueiredo, S. Nunes, E. Schlangen, J.L. Barroso-Aguiar, Durability of an UHPFRC under mechanical and chloride loads, Constr. Build. Mater. 311 (2021), 125223.

[5] Sohail, M. G.; Kahraman, R.; Al Nuaimi, N.; Gencturk, B.; Alnahhal, W., Durability characteristics of high and ultra-high performance concretes. *Journal of Building Engineering* **2021,** 33, 101669.

[6] A.M. Tahwia, G.M. Elgendy, M. Amin, Durability and microstructure of eco-efficient ultra-high-performance concrete, Constr. Build. Mater. 303 (2021), 124491.

[7] H. Martin-Sanz, E. Chatzi, E. Brühwiler, The use of Ultra High Performance Fibre Reinforced cement-based Composites in rehabilitation projects: a review. In Proceedings of the 9th International Conference on Fracture Mechanics of Concrete and Concrete Structures, 2016.

[8] Brühwiler, E. "Structural UHPFRC": Welcome to the post-concrete era! In International Interactive Symposium on Ultra-High Performance Concrete, 2016; Iowa State University Digital Press.

[9] D.-Y. Yoo, N. Banthia, Mechanical and structural behaviors of ultra-high-performance fiber-reinforced concrete subjected to impact and blast, Constr. Build. Mater. 149 (2017) 416–431.

[10] N. Bertola, P. Schiltz, E. Denarié, E. Brühwiler, A Review of the Use of UHPFRC in Bridge Rehabilitation and New Construction in Switzerland, Front. Built Environ. 7 (2021), 769686.

[11] E. Brühwiler, E. Denarié, Rehabilitation of concrete structures using ultra-high performance fibre reinforced concrete, University of Kassel (2008).

[12] Wibowo, H.; Sritharan, S. Use of ultra-high-performance concrete for bridge deck overlays; 2018.

[13] Plevny, Z., Applications of ultra-high performance concrete. **2020**.

[14] V. Perry, G. Weiss, Innovative field cast UHPC joints for precast bridge decks–Design, prototype testing and projects. In Proc., Int. Workshop of Designing and Building with Ultra-High Performance Fibre-Reinforced Concrete (UHPFRC), in: F. Toutlemonde, J. Resplendino (Eds.), State of the Art and Development, Wiley, Hoboken, NJ, 2009.

[15] P. Mazzacane, R. Ricciotti, G. Lamoureux, D. Corvez, Roofing of the Jean Bouin Stadium in UHPFRC, In RILEM-fib-AFGC Int. Symposium on Ultra-High Performance Fibre-Reinforced Concrete, UHPFRC, 2013.
[16] R. Ricciotti, R. Ricciotti, P. Mazzacane, The Enrico Navarra Gallery, Designing and Building with UHPFRC (2011) 79–86.
[17] Y. Voo, F.S. Malaysia, taking ultra-high performance concrete bridges to new dimensions. In Proceedings AFGC-ACI-fib-RILEM Int. Symposium on Ultra-High Performance Fibre-Reinforced Concrete, 2017.
[18] Buitelaar, P., Ultra-Thin Overlays with Hybrid Reinforced High Performance Concrete and Hybrid Reinforced Ultra High Performance Concrete. An unique rehabilitation system for industrial floors,-pavements and bridges.
[19] X. Shao, D. Yi, Z. Huang, H. Zhao, B. Chen, M. Liu, Basic performance of the composite deck system composed of orthotropic steel deck and ultrathin RPC layer, J. Bridge Eng. 18 (2013) 417–428.
[20] P.Y. Blais, C., M., prestressed pedestrian bridge: World's first Reactive Powder Concrete structure, PCI journal 44 (1999) 60–71.
[21] J. Resplendino, F. Toutlemonde, The UHPFRC revolution in structural design and construction. In International Symposium on Ultra-High Performance Fiber Reinforced Concrete, 2013.
[22] B. Vermeulen, Ultra High Performance Concrete in Action, Delft University of Technology, 2013.
[23] Brühwiler, E. Conceptual design and construction of lightweight R-UHPFRC bridges. In IABSE Symposium Report, 2017; International Association for Bridge and Structural Engineering.
[24] M. Luković, Literature review on new concrete types, Delft University of Technology, A start on exploring their opportunities for Dutch infrastructure, 2017.
[25] M. Bajaber, I. Hakeem, UHPC evolution, development, and utilization in construction: A review, J. Mater. Res. Technol. 10 (2021) 1058–1074.
[26] Du, J.; Meng, W.; Khayat, K. H.; Bao, Y.; Guo, P.; Lyu, Z.; Abu-obeidah, A.; Nassif, H.; Wang, H., New development of ultra-high-performance concrete (UHPC). *Composites Part B: Engineering* **2021,** 224, 109220.
[27] C.-C. Hung, S. El-Tawil, S.-H. Chao, A review of developments and challenges for UHPC in structural engineering: behavior, analysis, and design, J. Struct. Eng. 147 (2021) 03121001.
[28] B. Graybeal, E. Brühwiler, B.-S. Kim, F. Toutlemonde, Y.L. Voo, A. Zaghi, International perspective on UHPC in bridge engineering, J. Bridge Eng. 25 (2020) 04020094.
[29] AFGC, Bétons Fibrés à Ultra-Hautes Performances: Recommandations. Association Française de Génie Civil: Paris, France, 2013.
[30] H. Yokota, K. Rokugo, N. Sakata, JSCE recommendations for design and construction of high performance fiber reinforced cement composite with multiple fine cracks. In High Performance Fiber Reinforced Cement, Composites (2008).
[31] SIA, 2052: Béton fibré ultra-performant (BFUP)-Matériaux, dimensionnement et exécution. *Swiss Society of Engineers and Architects* **2016.**
[32] Y.L. Voo, S.J. Foster, C.C. Voo, Ultrahigh-performance concrete segmental bridge technology: Toward sustainable bridge construction, J. Bridge Eng. 20 (2015) B5014001.
[33] A.D. Reitsema, M. Luković, S. Grünewald, D.A. Hordijk, Future infrastructural replacement through the smart bridge concept, Materials 13 (2020) 405.
[34] R. Yu, Q. Song, X. Wang, Z. Zhang, Z. Shui, H. Brouwers, Sustainable development of Ultra-High Performance Fibre Reinforced Concrete (UHPFRC): Towards to an optimized concrete matrix and efficient fibre application, J. Cleaner Prod. 162 (2017) 220–233.
[35] K. Habel, Structural behaviour of elements combining ultra-high performance fibre reinforced concretes (UHPFRC) and reinforced concrete, EPFL (2004).
[36] T. Noshiravani, E. Brühwiler, Experimental investigation on reinforced ultra-high-performance fiber-reinforced concrete composite beams subjected to combined bending and shear, ACI Structural Journal 110 (2013) 251–261.
[37] M. Bastien-Masse, E. Brühwiler, Experimental investigation on punching resistance of R-UHPFRC–RC composite slabs, Mater. Struct. 49 (2015) 1573–1590.
[38] T.J. Mohammed, B.H. Abu Bakar, N. Muhamad Bunnori, Torsional improvement of reinforced concrete beams using ultra high-performance fiber reinforced concrete (UHPFC) jackets – Experimental study, Constr. Build. Mater. 106 (2016) 533–542.
[39] H. Yin, W. Teo, K. Shirai, Experimental investigation on the behaviour of reinforced concrete slabs strengthened with ultra-high performance concrete, Constr. Build. Mater. 155 (2017) 463–474.
[40] T. Zingaila, M. Augonis, M.R.T. Arruda, E. Šerelis, Š. Kelpša, Experimental and numerical analysis of flexural concrete-UHPFRC/RC composite members, Mechanics 23 (2017).
[41] S.A. Paschalis, A.P. Lampropoulos, O. Tsioulou, Experimental and numerical study of the performance of ultra high performance fiber reinforced concrete for the flexural strengthening of full scale reinforced concrete members, Constr. Build. Mater. 186 (2018) 351–366.
[42] Y. Zhu, Y. Zhang, H.H. Hussein, G. Chen, Flexural strengthening of reinforced concrete beams or slabs using ultra-high performance concrete (UHPC): A state of the art review, Eng. Struct. 205 (2020), 110035.
[43] Brühwiler, E.; Bastien-Masse, M.; Mühlberg, H.; Houriet, B.; Fleury, B.; Cuennet, S.; Schär, P.; Boudry, F.; Maurer, M. Strengthening the Chillon viaducts deck slabs with reinforced UHPFRC. In IABSE Symposium Report, 2015; International Association for Bridge and Structural Engineering.
[44] P.R. Prem, A.R. Murthy, Acoustic emission and flexural behaviour of RC beams strengthened with UHPC overlay, Constr. Build. Mater. 123 (2016) 481–492.
[45] M. Safdar, T. Matsumoto, K. Kakuma, Flexural behavior of reinforced concrete beams repaired with ultra-high performance fiber reinforced concrete (UHPFRC), Compos. Struct. 157 (2016) 448–460.
[46] B.A. Tayeh, B.H.A. Bakar, M.A. Megat Johari, A.M. Zeyad, Flexural Strength Behavior of Composite UHPFC – Existing Concrete, Adv. Mater. Res. 701 (2013) 32–36.
[47] L. Hussein, L. Amleh, Structural behavior of ultra-high performance fiber reinforced concrete-normal strength concrete or high strength concrete composite members, Constr. Build. Mater. 93 (2015) 1105–1116.
[48] K. Habel, E. Denarie, E. Bruhwiler, Structural response of elements combining ultrahigh-performance fiber-reinforced concretes and reinforced concrete, J Struct Eng-Asce 132 (2006) 1793–1800.
[49] A. Meda, G. Plizzari, Z. Rinaldi, G. Martinola, Strengthening of R/C existing columns with high performance fiber reinforced concrete jacket, in: C. Town, S. Africa (Eds.), In Proceedings of the 2nd international conference on concrete repair, rehabilitation and retrofitting, 2009.
[50] A.A. Bahraq, M.A. Al-Osta, S. Ahmad, M.M. Al-Zahrani, S.O. Al-Dulaijan, M. K. Rahman, Experimental and numerical investigation of shear behavior of RC beams strengthened by ultra-high performance concrete, Int. J. Concr. Struct. Mater. 13 (2019) 6.
[51] V. Garg, P.P. Bansal, R. Sharma, Retrofitting of Shear-Deficient RC Beams Using UHP-FRC, Ijst-T. Civ. Eng. 43 (2019) 419–428.
[52] M.A. Sakr, A.A. Sleemah, T.M. Khalifa, W.N. Mansour, Shear strengthening of reinforced concrete beams using prefabricated ultra-high performance fiber reinforced concrete plates: Experimental and numerical investigation, Struct. Concr. 20 (2019) 1137–1153.
[53] H. Ji, C. Liu, Ultimate shear resistance of ultra-high performance fiber reinforced concrete-normal strength concrete beam, Eng. Struct. 203 (2020), 109825.
[54] Lantsoght, E. O., How do steel fibers improve the shear capacity of reinforced concrete beams without stirrups? *Composites Part B: Engineering* **2019,** 175, 107079.
[55] P. Jongvivatsakul, L.V.H. Bui, T. Koyekaewphring, A. Kunawisarut, N. Hemstapat, B. Stitmannaithum, Using Steel Fiber-Reinforced Concrete Precast Panels for Strengthening in Shear of Beams: An Experimental and Analytical Investigation, Adv. Civ. Eng. 2019 (2019) 1–18.
[56] M. Bastien-Masse, E. Brühwiler, Composite model for predicting the punching resistance of R-UHPFRC–RC composite slabs, Eng. Struct. 117 (2016) 603–616.
[57] H. Youm, S. Hong, Evaluation for Punching Shear Strength of Slab-Column Connections with Ultra High Performance Fiber-Reinforced Concrete Overlay, Int. J. Struct. Eng. 12 (2018) 56–61.
[58] Masse, M. B.; Einpaul, J. Punching resistance of flat slabs strengthened with an added layer of UHPFRC. In IABSE Symposium Report, 2017; International Association for Bridge and Structural Engineering.
[59] X. Wu, S. Yu, S. Xue, T.-H.-K. Kang, H.-J. Hwang, Punching shear strength of UHPFRC-RC composite flat plates, Eng. Struct. 184 (2019) 278–286.
[60] E. Brühwiler, E. Denarié, Rehabilitation and Strengthening of Concrete Structures Using Ultra-High Performance Fibre Reinforced Concrete, Struct. Eng. Int. 23 (2018) 450–457.
[61] H. Yin, K. Shirai, W. Teo, Prediction of shear capacity of UHPC-concrete composite structural members based on existing codes, J. Civ. Eng. Manag. 24 (2018) 607–618.
[62] J.S. Engineers, o. C, Standard Specifications for Concrete Structures – 2007 "Design", JSCE Guidelines for concrete, Japan Society of Civil Engineers (2010).
[63] H. Yin, K. Shirai, W. Teo, Numerical model for predicting the structural response of composite UHPC–concrete members considering the bond strength at the interface, Compos. Struct. 215 (2019) 185–197.
[64] A. Committee, Building code requirements for structural concrete (ACI 318–08) and commentary, American Concrete Institute (2008).
[65] P. Code, Eurocode 2: design of concrete structures-part 1–1: general rules and rules for buildings, In British Standard Institution, London, 2005.
[66] A. c.,, Design considerations for steel fiber reinforced concrete. In, ACI Struct. J. (1988) 18.
[67] C.-F.-M. Code, CEB-FIB model code 2010–Final draft, In Thomas Thelford, Lausanne, Switzerland, 2010.
[68] T. Noshiravani, E. Brühwiler, Analytical Model for Predicting Response and Flexure-Shear Resistance of Composite Beams Combining Reinforced Ultrahigh Performance Fiber-Reinforced Concrete and Reinforced Concrete, J. Struct. Eng. 140 (2014).
[69] T. Noshiravani, E. Brühwiler, Rotation capacity and stress redistribution ability of R-UHPFRC–RC composite continuous beams: an experimental investigation, Mater. Struct. 46 (2013) 2013–2028.
[70] M. Bastien-Masse, E. Brühwiler, Contribution of R-UHPFRC strengthening layers to the shear resistance of RC elements, Struct. Eng. Int. 26 (2016) 365–374.
[71] Wuest, J. Comportement structural des bétons de fibres ultra performants en traction dans des éléments composés; EPFL: 2007.
[72] G. Ruano, F. Isla, D. Sfer, B. Luccioni, Numerical modeling of reinforced concrete beams repaired and strengthened with SFRC, Eng. Struct. 86 (2015) 168–181.
[73] M.A. Tathagata Bhaduri, Modeling of Steel Reinforced Ultra-High-Performance Concrete (UHPC) Beams Failure, In Second International Interactive Symposium on Ultra-High Performance Concrete, Albany, NY, USA, 2019.
[74] H.H. Dinh, Shear behavior of steel fiber reinforced concrete beams without stirrup reinforcement, University of Michigan, 2009.
[75] M.A. Sakr, S.R. El-khoriby, T.M. Khalifa, M.T. Nagib, Modeling of RC shear walls strengthened with ultra-high performance fiber reinforced concrete (UHPFRC) jackets, Eng. Struct. 200 (2019), 109696.

[76] G. Martinola, A. Meda, G.A. Plizzari, Z. Rinaldi, Strengthening and repair of RC beams with fiber reinforced concrete, Cem. Concr. Compos. 32 (2010) 731–739.
[77] M.A. Al-Osta, M.N. Isa, M.H. Baluch, M.K. Rahman, Flexural behavior of reinforced concrete beams strengthened with ultra-high performance fiber reinforced concrete, Constr. Build. Mater. 134 (2017) 279–296.
[78] A. Momayez, M.R. Ehsani, A.A. Ramezanianpour, H. Rajaie, Comparison of methods for evaluating bond strength between concrete substrate and repair materials, Cem. Concr. Res. 35 (2005) 748–757.
[79] C. Zanotti, N. Randl, Are concrete-concrete bond tests comparable? Cem. Concr. Compos. 99 (2019) 80–88.
[80] N. Randl, Design recommendations for interface shear transfer in fib Model Code 2010, Struct. Concr. 14 (2013) 230–241.
[81] D. Morgan, Compatibility of concrete repair materials and systems, Constr. Build. Mater. 10 (1996) 57–67.
[82] Lukovic, M.; Ye, G.; Van Breugel, K. Reliable concrete repair: A critical review. In 14th International Conference Structural Faults and Repair, Edinburgh, Scotland, UK, 3-5 July 2012, 2012.
[83] A. Abu-Tair, S. Rigden, E. Burley, Testing the bond between repair materials and concrete substrate, ACI Mater. J. 93 (1996) 553–558.
[84] S. Austin, P. Robins, Y.G. Pan, Shear bond testing of concrete repairs, Cem. Concr. Res. 29 (1999) 1067–1076.
[85] M. Naderi, Effects of cyclic loading, freeze-thaw and temperature changes on shear bond strengths of different concrete repair systems, J. Adhes. 84 (2008) 743–763.
[86] R.-D. López-Carreño, P. Pujadas, S.H.P. Cavalaro, A. Aguado, Bond strength of whitetoppings and bonded overlays constructed with self-compacting high-performance concrete, Constr. Build. Mater. 153 (2017) 835–845.
[87] D.P. Bentz, I. De la Varga, J.F. Muñoz, R.P. Spragg, B.A. Graybeal, D.S. Hussey, D. L. Jacobson, S.Z. Jones, J. LaManna, M., Influence of substrate moisture state and roughness on interface microstructure and bond strength: Slant shear vs. pull-off testing, Cem. Concr. Compos. 87 (2018) 63–72.
[88] C. Zanotti, N. Banthia, G. Plizzari, A study of some factors affecting bond in cementitious fiber reinforced repairs, Cem. Concr. Res. 63 (2014) 117–126.
[89] B.A. Tayeh, B.H. Abu Bakar, M.A. Megat Johari, Characterization of the interfacial bond between old concrete substrate and ultra high performance fiber concrete repair composite, Mater. Struct. 46 (2012) 743–753.
[90] B.A. Tayeh, B.H. Abu Bakar, M.A. Megat Johari, Y.L. Voo, Mechanical and permeability properties of the interface between normal concrete substrate and ultra high performance fiber concrete overlay, Constr. Build. Mater. 36 (2012) 538–548.
[91] Z.B. Haber, J.F. Munoz, I. De la Varga, B.A. Graybeal, Bond characterization of UHPC overlays for concrete bridge decks: Laboratory and field testing, Constr. Build. Mater. 190 (2018) 1056–1068.
[92] P. Ganesh, A. Ramachandra Murthy, Simulation of surface preparations to predict the bond behaviour between normal strength concrete and ultra-high performance concrete, Constr. Build. Mater. 250 (2020).
[93] A.A. Semendary, D. Svecova, Factors affecting bond between precast concrete and cast in place ultra high performance concrete (UHPC), Eng. Struct. 216 (2020), 110746.
[94] S. Austin, P. Robins, Y.G. Pan, Tensile Bond Testing of Concrete Repairs, Mater. Struct. 28 (1995) 249–259.
[95] K.N. Bakhsh, Evaluation of bond strength between overlay and substrate in concrete repairs, Architecture and the Built Environment, KTH Royal Institute of Technology, 2010.
[96] M. Valipour, K.H. Khayat, Debonding test method to evaluate bond strength between UHPC and concrete substrate, Mater. Struct. 53 (2020) 15.
[97] A.D. Espeche, J. León, Estimation of bond strength envelopes for old-to-new concrete interfaces based on a cylinder splitting test, Constr. Build. Mater. 25 (2011) 1222–1235.
[98] J. Silfwerbrand, Shear bond strength in repaired concrete structures, Mater. Struct. 36 (2003) 419–424.
[99] A. Valikhani, A.J. Jahromi, I.M. Mantawy, A. Azizinamini, Experimental evaluation of concrete-to-UHPC bond strength with correlation to surface roughness for repair application, Constr. Build. Mater. 238 (2020).
[100] Y. Zhang, C. Zhang, Y. Zhu, J. Cao, X. Shao, An experimental study: various influence factors affecting interfacial shear performance of UHPC-NSC, Constr. Build. Mater. 236 (2020), 117480.
[101] M. Chestney, Concrete Patch Repair Bond Strength, Loughborough University, Department of Civil Building Engineering, 1996.
[102] M. Farzad, M. Shafieifar, A. Azizinamini, Experimental and numerical study on bond strength between conventional concrete and Ultra High-Performance Concrete (UHPC), Eng. Struct. 186 (2019) 297–305.
[103] F. Perez, B. Bissonnette, R. Gagné, Parameters affecting the debonding risk of bonded overlays used on reinforced concrete slab subjected to flexural loading, Mater. Struct. 42 (2009) 645–662.
[104] O.T. Tsioulou, A.P. Lampropoulos, S.E. Dritsos, Experimental investigation of interface behaviour of RC beams strengthened with concrete layers, Constr. Build. Mater. 40 (2013) 50–59.
[105] Tayeh, B. A.; Bakar, B. A.; Johari, M. M. Mechanical properties of old concrete—UHPFC interface. In Concrete Repair, Rehabilitation and Retrofitting III: 3rd International Conference on Concrete Repair, Rehabilitation and Retrofitting, ICCRRR-3, 3-5 September 2012, Cape Town, South Africa, 2012; CRC Press.
[106] F.J. Alaee, B.L. Karihaloo, Retrofitting of reinforced concrete beams with CARDIFRC, J. Compos. Constr. 7 (2003) 174–186.
[107] H.M. Tanarslan, N. Alver, R. Jahangiri, Ç. Yalçınkaya, H. Yazıcı, Flexural strengthening of RC beams using UHPFRC laminates: Bonding techniques and rebar addition, Constr. Build. Mater. 155 (2017) 45–55.
[108] M. Kazemi Kamyab, Autogenous Shrinkage and Hydration Kinetics of SH-UHPFRC under Moderate to Low Temperature Curing Conditions, EPFL (2013).
[109] L. Courard, Adhesion of repair systems to concrete: Influence of interfacial topography and transport phenomena, Mag. Concr. Res. 57 (2005) 273–282.
[110] L. Courard, T. Piotrowski, A. Garbacz, Near-to-surface properties affecting bond strength in concrete repair, Cem. Concr. Compos. 46 (2014) 73–80.
[111] L. Courard, Parametric study for the creation of the interface between concrete and repair products, Mater. Struct. 33 (2000) 65.
[112] M. Lukovic, G. Ye, Effect of moisture exchange on interface formation in the repair system studied by X-ray absorption, Materials 9 (2016) 2.
[113] J. Zhou, G. Ye, K. van Breugel, Cement hydration and microstructure in concrete repairs with cementitious repair materials, Constr. Build. Mater. 112 (2016) 765–772.
[114] Y. Chen, F. Matalkah, W. Rankothge, A. Balachandra, P. Soroushian, Improvement of the surface quality and aesthetics of ultra-high-performance concrete, Proceedings of the Institution of Civil Engineers-Construction Materials 172 (2019) 246–255.
[115] M. Kazemi Kamyab, E. Denarié, E. Brühwiler, B. Wang, M. Thiéry, P.F. Faure, V. Baroghel-Bouny, Characterization of moisture transfer in UHPFRC-concrete composite systems at early age. In Proceedings of the 2nd International Conference on Microstructural-related Durability of Cementitious Composites, 2012.
[116] M. Luković, G. Ye, E. Schlangen, K. Van Breugel, Moisture movement in cement-based repair systems monitored by X-ray absorption, Heron 62 (2017) 21.
[117] Y. Zhang, P. Zhu, Z. Liao, L. Wang, Interfacial bond properties between normal strength concrete substrate and ultra-high performance concrete as a repair material, Constr. Build. Mater. 235 (2020).
[118] G. Martinola, H. Sadouki, F.H. Wittmann, Numerical model for minimizing risk of damage in repair system, J. Mater. Civ. Eng. 13 (2001) 121–129.
[119] W. Li, Z. Huang, G. Hu, W.H. Duan, S.P. Shah, Early-age shrinkage development of ultra-high-performance concrete under heat curing treatment, Constr. Build. Mater. 131 (2017) 767–774.
[120] D.-Y. Yoo, N. Banthia, Y.-S. Yoon, Geometrical and boundary condition effects on restrained shrinkage behavior of UHPFRC slabs, KSCE J. Civ. Eng. 22 (2017) 185–195.
[121] K. Habel, J.-P. Charron, E. Denarié, E. Brühwiler, Autogenous deformations and viscoelasticity of UHPFRC in structures. Part I: experimental results, Mag. Concr. Res. 58 (2006) 135–145.
[122] D.-Y. Yoo, N. Banthia, Mechanical properties of ultra-high-performance fiber-reinforced concrete: A review, Cem. Concr. Compos. 73 (2016) 267–280.
[123] T. Xie, C. Fang, M.M. Ali, P. Visintin, Characterizations of autogenous and drying shrinkage of ultra-high performance concrete (UHPC): An experimental study, Cem. Concr. Compos. 91 (2018) 156–173.
[124] Tsioulou, O. T.; Agaoglu, C.; Lampropoulos, A. P. Restrained concrete shrinkage effect on Concrete Elements strengthened with UHPFRC layers. In 20th Congress of IABSE, New York City 2019: The Evolving Metropolis-Report, 2019; IABSE (International Association for Bridge and Structural Engineering).
[125] K. Habel, E. Denarié, E. Brühwiler, Time dependent behavior of elements combining ultra-high performance fiber reinforced concretes (UHPFRC) and reinforced concrete, Mater. Struct. 39 (2006) 557–569.
[126] Y. Zhu, Y. Zhang, H.H. Hussein, J. Liu, G. Chen, Experimental study and theoretical prediction on shrinkage-induced restrained stresses in UHPC-RC composites under normal curing and steam curing, Cem. Concr. Compos. 103602 (2020).
[127] M.A. Carbonell Muñoz, D.K. Harris, T.M. Ahlborn, D.C. Froster, Bond performance between ultrahigh-performance concrete and normal-strength concrete, J. Mater. Civ. Eng. 26 (2014) 04014031.
[128] B.A. Tayeh, B.A. Bakar, M.M. Johari, Y.L. Voo, Utilization of ultra-high performance fibre concrete (UHPFC) for rehabilitation–a review, Procedia Eng. 54 (2013) 525–538.
[129] J.P. Charron, E. Denarie, E. Bruhwiler, Transport properties of water and glycol in an ultra high performance fiber reinforced concrete (UHPFRC) under high tensile deformation, Cem. Concr. Res. 38 (2008) 689–698.
[130] R.J. Torrent, A two-chamber vacuum cell for measuring the coefficient of permeability to air of the concrete cover on site, Mater. Struct. 25 (1992) 358–365.
[131] B.A. Graybeal, Material property characterization of ultra-high performance concrete; United States. Federal Highway Administration, Office of Infrastructure Research and Development. (2006).
[132] L. Guingot, D. Dekhil, P. Soulier, Strengthening of hydraulic structures with UHPC. In Proceedings of RILEM-fib-AFGC International Symposium on Ultra-High Performance Fibre-Reinforced Concrete, 2013.
[133] Denarié, E.; Jacomo, D.; Fady, N.; Corvez, D. Rejuvenation of maritime signalisation structures with UHPFRC; 2013.
[134] H. Sadouki, E. Denarié, E. Brühwiler, Validation of a FEA model of structural response of RC-cantilever beams strengthened with a (R-) UHPFRC layer, Constr. Build. Mater. 140 (2017) 100–108.
[135] A.P. Lampropoulos, S.A. Paschalis, O.T. Tsioulou, S.E. Dritsos, Strengthening of reinforced concrete beams using ultra high performance fibre reinforced concrete (UHPFRC), Eng. Struct. 106 (2016) 370–384.
[136] Du béton, F., Structural Connections for Precast Concrete Buildings: Guide to Good Practice, International Federation for Structural Concrete (fib) (2008).

[137] Y. Zhu, Y. Zhang, H.H. Hussein, G. Chen, Numerical modeling for damaged reinforced concrete slab strengthened by ultra-high performance concrete (UHPC) layer, Eng. Struct. 209 (2020), 110031.
[138] AASHTO, L., American Association of State Highway and Transportation Officials Load-and-resistance factor design. Washington, DC: 2017.
[139] ACI, Building code requirements for structural concrete and commentary. 2011.
[140] A. Muttoni, Punching shear strength of reinforced concrete slabs without transverse reinforcement, ACI Struct. J. 4 (2008) 440–450.
[141] Noshiravani, T. Structural Response of R-UHPFRC-RC Composite Members Subjected to Combined Bending and Shear; EPFL: 2012.
[142] Z. Lin, Y. Liu, J. He, Behavior of stud connectors under combined shear and tension loads, Eng. Struct. 81 (2014) 362–376.
[143] M.G. Alexander, M.A. Sakr, A.A. Sleemah, T.M. Khalifa, W.N. Mansour, H. Beushausen, F. Dehn, P. Moyo, Behavior of RC beams strengthened in shear with ultra-high performance fiber reinforced concrete (UHPFRC), MATEC Web of Conferences 199 (2018).